

博士論文

網膜内活性化マイクログリアの機能解析

森内 裕太

## Table of Contents

Abstract.....	2
Introduction .....	4
Methods .....	23
Results .....	30
Discussion.....	65
Acknowledgments .....	73
References .....	73

## Abstract

Microglia are tissue-resident macrophage-like cells in the central nervous system (CNS) and play roles in regulating immune responses in the CNS<sup>1</sup>. Microglia undergo activation by retinal degeneration but the role of activated microglia remains poorly understood in retinal degeneration. Several different cell types including microglia and Müller glia play roles to form pathology of retinal degeneration, and it is difficult to evaluate the roles of microglia in complex situations. Microglial activation are regulated by Colony stimulating factor 1 receptor (CSF1R), Fc gamma receptor (FcγR), and TREM2, which have the Ras signaling pathway as a downstream signaling pathway<sup>2-4</sup>. I aimed to activate microglia by activating Ras signaling in microglia and expressed RasV12, a constitutive active form of Ras, in microglia using transgenic mice to exactly evaluate the roles of activated microglia in the retina. Ras activated microglia induced not only microglial proliferation, morphological changing, and accumulation in the outer/ inner sides of the retina (Fig. 1A), but induced photoreceptor-specific degeneration accompanied by exposure of phosphatidylserine (PS) on extracellular membrane and phagocytosis of photoreceptors by Ras activated microglia (Fig. 1B, C). Also, Ras activated microglia Müller glial activation, upregulation of photoreceptor injury-related genes: *Edn2* and *Fgf2*, and activated microglia-related genes: *Il1b*, *Il6*, and *Tnf*, suggesting that activation of retinal inflammatory circuits are activated by Ras activation in microglia (Fig. 1C). These findings indicated that activated microglia trigger photoreceptor degeneration.

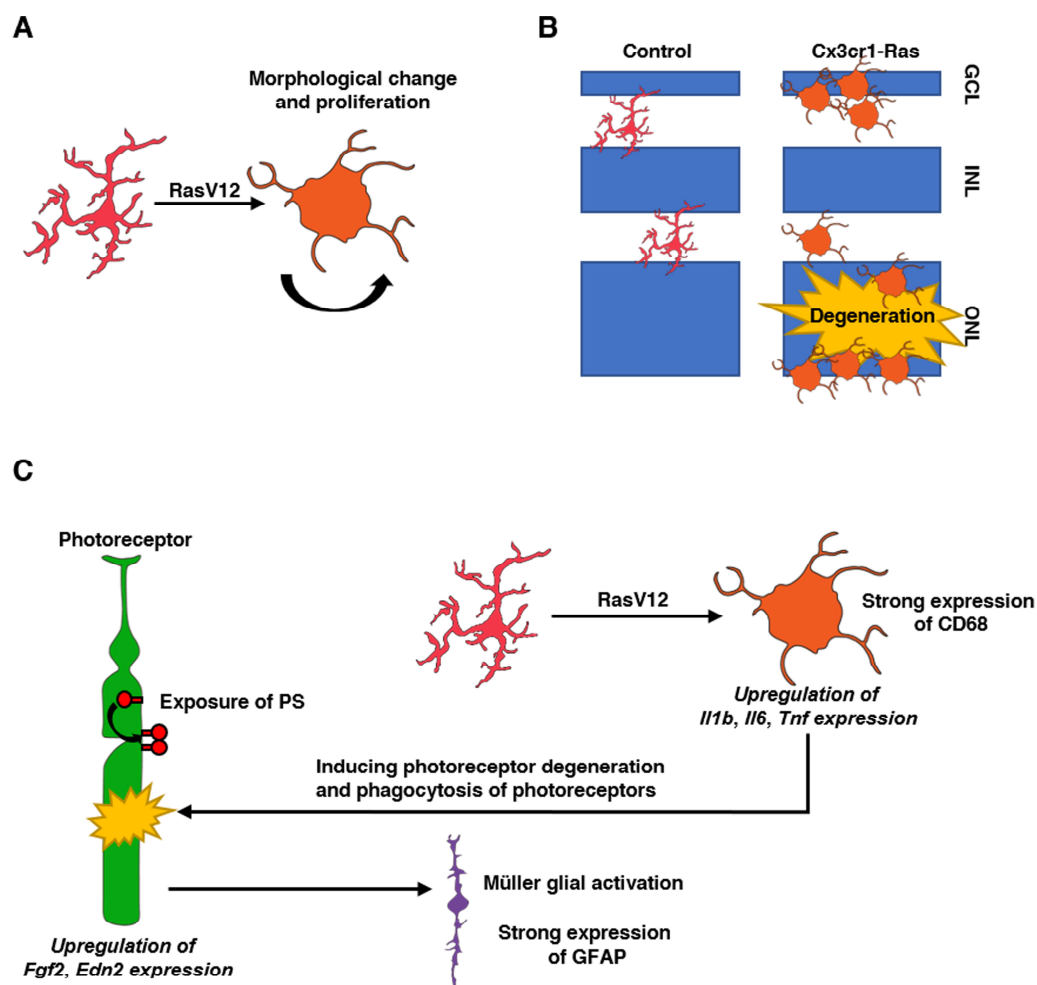


**Figure 1 Graphical Abstracts**

(A) RasV12 expression in microglia induced morphological change and proliferation. (B) RasV12 expressed microglia accumulation in the outer/ inner sides of the retina and induced photoreceptor-specific degeneration. (C) Cx3cr1-Ras mice showed activation of retinal inflammatory circuits. RasV12 expression in microglia upregulated *Il1b*, *Il6*, and *Tnf* expression, and also showed phagocytosis of photoreceptors. The Cx3cr1-Ras mice showed Müller glial activation accompanied with strong GFAP expression, and exposure of phosphatidylserine (PS) on photoreceptors and upregulation of photoreceptor injury-related genes: *Edn2* and *Fgf2*.



## **Introduction**

### ***Preface***

I examined the roles of activated microglia in the retina *in vivo* using newly established microglia activating model and inhibitory effects of IL-33 on the activated microglia. In this section, I describe the background, previous studies, and the aim of this study.

### ***Retinal Structure, Component Cells, Function, and Features***

The retina is a part of the central nervous system (CNS) and plays essential roles in animals by transducing light signal to an electric signal. The retina consists of three layers of cell bodies and two layers of nerve fibers and synapses: the inner plexiform layer (IPL) and outer plexiform layer (OPL). The ganglion cell layer (GCL) contains retinal ganglion cells. The inner nuclear layer (INL) contains horizontal cells, amacrine cells, bipolar cells, and Müller glial cells. The outer nuclear layer (ONL) contains rod and cone photoreceptors. The subretinal (SR) region contains inner and outer segments of photoreceptors and retinal pigment epithelium (RPE). Microglia exist in the IPL and OPL (Fig. 2). The light signal is converted to an electric signal by rod and cone photoreceptors. The electric signals from photoreceptors are transmitted to retinal ganglion cells via bipolar cells. The retinal ganglion cells transmit signals to the brain by axial fiber. Horizontal cells and amacrine cells are involved in horizontal interaction of photoreceptor and retinal ganglion cells, respectively <sup>5</sup>. The RPE is involved in the maintenance of photoreceptors by transporting growth factors and eliminating waste materials <sup>6</sup>. The retina is one of the immune privilege sites such as the brain and spinal cord, which are defined as physical barriers preventing free bacteria, molecules, and circulating immune cells in blood <sup>7, 8, 9</sup>. RPEs also construct blood-retinal barrier (BRB) by forming tight junctions each other and block infiltration of immune cells <sup>10</sup> except in RPE degenerative condition. The main player of retinal immune systems is microglia in an early-onset of retinal degeneration.

Feature of the retina is characterized by receiving environmental insults which is distinct from other CNS belonging tissues. Photoreceptors are transduced from light signal to electric signal via phototransduction cascade <sup>11</sup> and constitutively receiving phototoxic damage, in which is one of the risk factors for age-related macular degeneration (AMD) <sup>12</sup>.

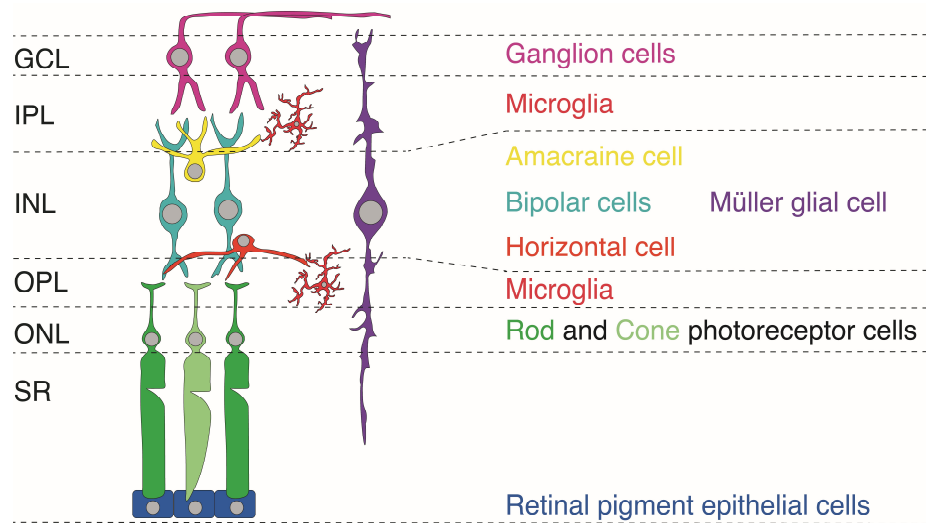


**Figure 2 The structure of the mammalian retina**

The retina consists of three layers of cell bodies and two layers of nerve fibers and synapses; inner plexiform layer (IPL) and outer plexiform layer (OPL). The ganglion cell layer (GCL) contains retinal ganglion cells. The inner nuclear layer (INL) contains horizontal cells, amacrine cells, bipolar cells, and Müller glial cells. The outer nuclear layer (ONL) contains rod and cone photoreceptors. Microglia exist in IPL and OPL. The subretinal region (SR) contains outer segments of photoreceptors cells and retinal pigment epithelial cells. The picture was adopted from The Retina: Retinal Layers, Variant Image ID: 29736; <https://www.netterimages.com/the-retina-retinal-layers-labeled-felten-2e-29736.html> and was drawn by Moriuchi.

### ***Retinitis Pigmentosa***

Retinal degenerative diseases include retinitis pigmentosa, age-related macular degeneration, Stargardt disease, cone-rod photoreceptor dystrophy, and glaucoma. Most of the retinal degenerative diseases are accompanied by photoreceptor selective degeneration. In this part, I summarized the futures of retinitis pigmentosa (RP) as a typical example of photoreceptor degenerative disease. RP is an inherited degenerative disease characterized by selective degeneration of rod photoreceptors and leads to progressive tunnel vision and visual loss <sup>13</sup>. The symptoms of RP are mainly caused by rod photoreceptor degeneration. Histological sections from RP patients show reduction of ONL and photoreceptor outer segments thickness which are caused by photoreceptor selective degeneration <sup>14</sup>. The age of onset of RP is middle age of the life. Indeed, the number of RP patients increases at the age of 40s to 50s <sup>15, 16</sup>. Therefore, aging is one of the key factors of RP onset and progression. Over forty gene mutations are identified as causal genes with their mutation, and relatively frequent genes are such as *Eys*, *Rpgr*, *Rho*, *Pde6b*, and *Rpl* <sup>13</sup>. Most of the genes are responsible for the visual cycle and maintenance of photoreceptors, and RPEs. However, gene mutations have not identified with over 50 percent of Japanese RP patients, suggesting requirement of more large-scale examination of whole genome of the patients (Fig. 3).

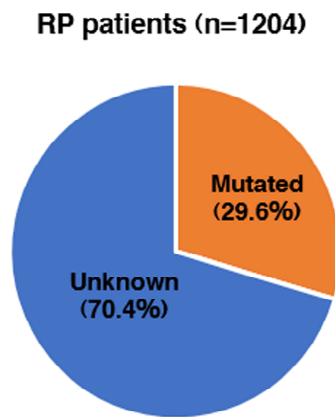


***Figure 3 Genetic profile of retinitis pigmentosa (RP)-related genes in 1204 Japanese RP patients***

29.6% of patients have mutation in RP-related genes including *Eys*, *Rpgp*, *Rho*, *Pde6b*, and, *Rpl*. However, 70.4% of RP patients do not have gene mutations in the RP-related genes <sup>13</sup>. The pie chart was adopted from Koyanagi et al., Journal of Medical Genetics, 2019.

### ***Animal Models for Retinitis Pigmentosa (RP)***

#### **N-Methyl-N-Nitrosourea (MNU) Treatment Model**

MNU treatment model is widely used as a pharmaceutical induction model for RP. MNU is an alkylating agent, which can induce photoreceptor specific apoptosis by injecting intraperitoneally in adult mice<sup>17, 18</sup>. MNU-injected mice are shown photoreceptor degeneration from 4 days post injection, and significant reduction was observed in the ONL thickness at 7 days post injection. Microglia and Müller glial cells are activated from 4 days post injection. Also, MNU-injected mice show microglial accumulation in the ONL like RP patient specimens. MNU is known to induce DNA damages by chemical modification of DNA but molecular mechanisms of MNU-inducing photoreceptor degeneration has been still unclear<sup>18</sup>.

#### **Retinal Degeneration 10 (rd10) Mouse**

Rd10 mouse is a model for autosomal recessive RP, which contains a mutation in rod photoreceptor's cGMP phosphodiesterase  $\beta$  subunit (*Pde6b*). Rd10 eye shows rod photoreceptor degeneration and microglial activation from postnatal day 14<sup>19, 20</sup>. The mice show loss of rod photoreceptors by 2 months old.

### ***Microglial Development and Function in the Healthy Retina and Brain***

Microglia are tissue-resident macrophage-like cells in the CNS and play roles in regulating immune responses in the CNS<sup>1</sup>. In both mouse retina and brain, microglia develop during the early period of embryogenesis and migrate to the CNS. The origin of microglia is erythromyeloid progenitor (EMP) in yolk sac blood islands. The EMPs differentiate to early microglia in yolk sac blood islands and migrate toward CNS at embryonic days 9.5<sup>21, 22</sup>. Colony stimulating factor 1 receptor (CSF1R), a receptor for CSF1 and IL-34, transmits signaling necessary for microglial survival and proliferation in the adult retina. A recent study reported that microglial survival depended on IL-34 in

the IPL, whereas did not depend on IL-34 in the OPL under the non-inflammatory condition <sup>21</sup>. In the healthy retina and brain, microglia involve in keeping homeostasis of neurons and synaptic transmission by clearing dead neurons and secreting neurotrophic factors <sup>18, 19</sup>. Resting microglia shows ramified morphology which has a much long foot process and small cellular body in the non-inflammatory and non-degenerated conditions.

### ***Microglial Activation in the CNS***

Microglial activation is induced by not only in retinal degeneration diseases but also in other CNS degeneration or injury diseases including Alzheimer's disease, amyotrophic lateral sclerosis, multiple sclerosis, neuropathic pain <sup>25</sup>, and traumatic brain injury <sup>26</sup>. In the neurodegenerative diseases, activated microglia are expected to have neuroprotective or neurodegenerative effects, but how they modulate pathology is still largely unknown. Microglial activation is caused by damage-associated molecular patterns (DAMPs) from dead neural cells <sup>27, 28</sup>, and pathological proteins for example amyloid- $\beta$ , tau-protein <sup>29</sup>, <sup>30</sup>. Microglia undergo morphological change from ramified morphology to ameboid morphology when they are activated. Activated microglia show two different phenotypes that are inflammatory phenotype (M1 phenotype) and anti-inflammatory phenotype (M2 phenotype). Activated microglia by LPS, amyloid- $\beta$ , apolipoprotein e (ApoE), and DAMPs, show M1 phenotype and secrete inflammatory factors (e.g. IL-1 $\beta$ , IL-6, TNF- $\alpha$ , and nitric oxide). M1 activated microglia are involved in inducing of neurodegeneration and inflammatory, and are characterized by upregulation of *Il1b*, *Il6*, *Tnf* gene expression, and inducible nitric oxide synthase (iNOS) protein expression. In contrast, activation of microglia by IL-4, IL-10, IL-13, and TGF- $\beta$  leads to M2 phenotype that is characterized by secretion of anti-inflammatory factors (e.g. IL-4, IL-10, and TGF- $\beta$ ) and neuro neurotrophic factors (e.g. BDNF and IGF-1). M2 activated microglia are involved in neuroprotection and suppress M1 activated microglia induced inflammatory.

M2 microglia are characterized by upregulation of *Il4*, *Il10*, *Tgfb1*, and *Bdnf* gene expression and Arginase-1 (Arg 1) protein expression.<sup>27, 28</sup> (Fig. 4).



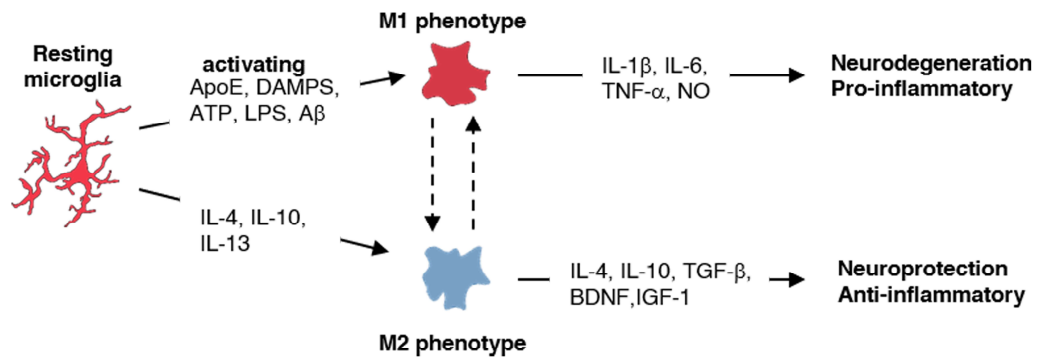


**Figure 4 Activated microglia shows inflammatory phenotype (M1 phenotype) or anti-inflammatory phenotype (M2 phenotype).**

Resting microglia are activated by extracellular factors. Activated microglia shows M1 phenotype or M2 phenotype. Activated microglia by LPS, amyloid- $\beta$ , apolipoprotein e (ApoE), and DAMPs, shows M1 phenotype and secrete inflammatory factors (e.g. IL-1 $\beta$ , IL-6, TNF- $\alpha$ , and nitric oxide (NO)). M1 activated microglia are involved in inducing neurodegeneration and inflammation. In contrast, activated microglia by IL-4, IL-10, IL-13, and TGF- $\beta$  shows M2 phenotype and secrete anti-inflammatory factors (e.g. IL-4, IL-10, and TGF- $\beta$ ) and neurotrophic factors (e.g. BDNF and IGF-1). M2 activated microglia are involved in neuroprotection and anti-inflammation.

### ***Roles of Microglia in the Retinitis Pigmentosa (RP)***

In the human, late-onset concentric RP patient shows that activated microglia accumulate in the ONL and SR especially in the photoreceptor degenerated regions, and seems to clear photoreceptor cell debris <sup>31</sup>. Activated microglia interact with degenerated photoreceptors but studies of activated microglia using RP patient specimen are limited. Recently, several studies demonstrated the roles of activated microglia using RP animal models. In the rd10 mouse model, microglia are activated by photoreceptor apoptosis, and contributed to the aggravation of photoreceptor degeneration by an IL-1 $\beta$ -dependent manner and phagocytosing stressed living photoreceptors <sup>32</sup>. Consistently, depletion of microglia by using genetic <sup>32</sup> or pharmaceutical models <sup>33</sup> are recovered photoreceptor degeneration in the rd10 mouse model. However, the roles of microglia in the photoreceptor degenerative conditions are still controversial because previous studies focusing on secondary effects of activated microglia or late-onset of photoreceptor degeneration.

### ***Microglia in Aged CNS***

In the aged mice and human brain, microglia upregulate inflammatory factors including IL-1 $\beta$ , IL-6, and nitric oxide, whereas downregulate anti-inflammatory factors including IL-4 and IL-10 <sup>34</sup>. Studies of the human healthy aged retina are limited, but several studies using the aged mice had been reported. In the aged mice retina, microglia shows the ameboid shape and accumulate in SR <sup>35</sup>. Furthermore, RNA-seq analysis of isolated microglia from healthy aged mice retina showed that enrichment of microglial immune function and regulation related genes, which are relating IL-1, IL-3, and nitric oxide signaling. LPS-stimulated Ras-MAPK signaling pathway is also activated, and *Cfb* and *C3*, age-related macular degeneration related genes are significantly upregulated in microglia from aged retina <sup>36</sup>. Therefore, microglia enhance the inflammatory status, and chronic inflammatory status are related to neurodegenerative diseases in the aged brain and

retina.

### ***Retinal Inflammatory Circuits***

The retina has complex immune circuits, in which activating photoreceptor degeneration. Injured or degenerated photoreceptors secrete alarmins (e.g. endothelin-2: EDN2 <sup>37</sup>, DAMPs, and ATP <sup>38</sup>. The alarmins activate Müller glia. The activated Müller glia secrete factors including leukemia inhibitory factor (LIF) and protect photoreceptor from degeneration by upregulating neuroprotective factor: FGF2 <sup>39, 40</sup>. The alarmins also activate microglia. Activated microglia secrete inflammatory factors such as IL-1 $\beta$ , IL-6, TNF- $\alpha$ , and nitric oxide (NO) <sup>38</sup> and induce aggravating photoreceptor degeneration (Fig. 5).

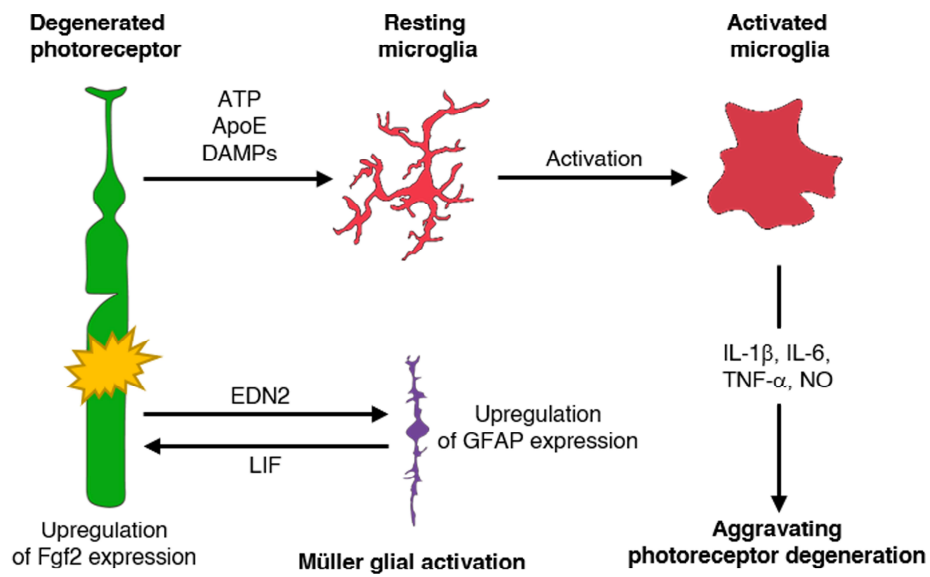


**Figure 5 Inflammatory circuits in the photoreceptor degenerated retina.**

Retina has complex immune circuits that are activated by photoreceptor degeneration. Injured or degenerated photoreceptors secrete the alarmins such as Endothelin-2 (EDN2), damage-associated molecular patterns (DAMPs), and ATP. The alarmins activate microglia and Müller glial cells. Activated microglia secrete inflammatory factors such as IL-1 $\beta$ , IL-6, TNF- $\alpha$ , and nitric oxide (NO) and are involved in aggravating photoreceptor degeneration. The activated Müller glia secrete factors including leukemia inhibitory factor (LIF) and protect photoreceptor from degeneration by upregulating neuroprotective factor: FGF2.

### ***Ras Signaling Pathway***

Ras, a small G-protein, is a signal transducer that has guanosine diphosphate (GDP)-binding active form and guanosine triphosphate (GTP)-binding active form. Ras activation is regulated GDP/ GTP binding by guanine nucleotide exchange-factors (GEFs) and GTPase-activating proteins (GAPs) <sup>41</sup>. GEFs activate Ras by converting Ras binding GDP to GTP, whereas GAPs inactivate Ras by hydrolyzing Ras binding GTP to GDP (Fig. 6A). The Ras has four isoforms: H-Ras, N-Ras, K-Ras4a and K-Ras4b and they share 82% sequence in the GTPase domain <sup>41</sup>. Ras has several downstream signaling pathways, including the Raf/ Mek/ Erk (MAPK cascade), phosphatidylinositol-3 kinase (PI3K)-Akt, and Phospholipase C (PLC) signaling pathways (Fig. 6B) <sup>42</sup>. K-Ras is activated by microglial regulation related receptors, including CSF1R, Fc gamma receptor (FcγR), and TREM2 (Fig. 6B) <sup>2-4</sup>. Because Ras activates proliferation-related signaling pathways such as the MAPK pathway as a downstream signaling pathway, mutations of Ras are reported in various cancers (e.g. colon, breast, brain, kidney, lung, and so on), and most of the mutation sites are G12, G13, and Q61 <sup>43</sup>. One of the mutated Ras has a substitution of G12 with V (RasV12) which disrupts the GTP- GTPase domain of GAPs interaction (Fig. 6C) <sup>43</sup>. Therefore, RasV12 mutant induces constitutive activation of Ras and aberrant cell proliferation.

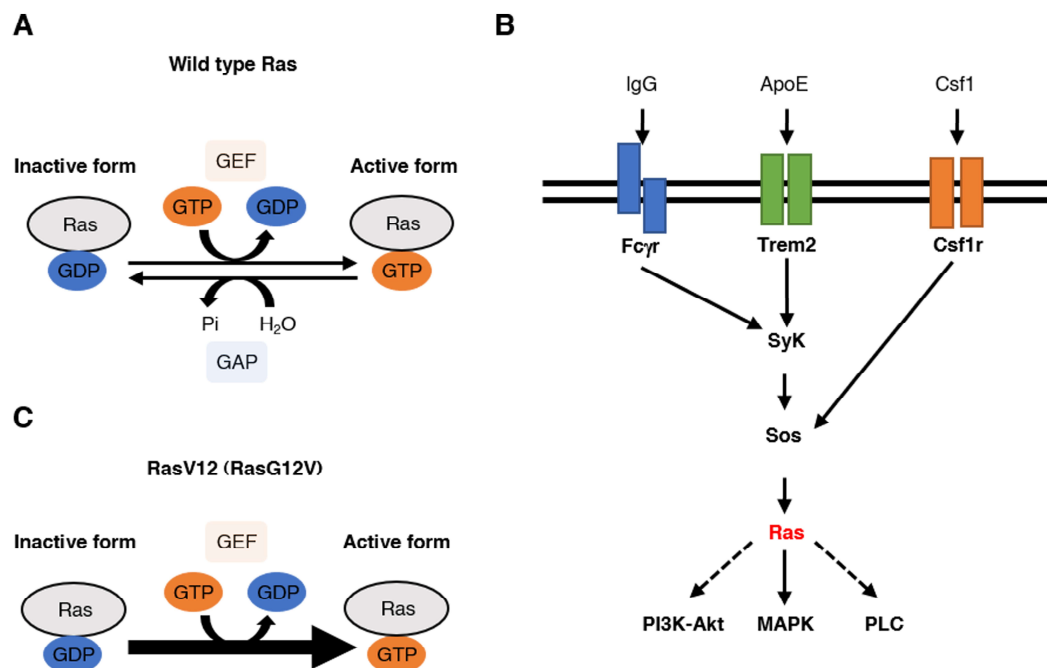


**Figure 6 Regulation of Ras and Ras signaling pathway.**

(A) Regulation of Ras by guanine nucleotide exchange-factors (GEFs) and GTPase-activating proteins (GAPs). The Ras has guanosine diphosphate (GDP)-binding active form and guanosine triphosphate (GTP)-binding active form. Ras activation is regulated GDP/ GDP binding by guanine nucleotide exchange-factors (GEFs) and GTPase-activating proteins (GAPs)<sup>41</sup>. GEFs are activate Ras by converting Ras binding GDP to GTP, whereas GAPs are inactive Ras by hydrolyzing Ras binding GTP to GDP (B) The signaling pathway of Ras. K-Ras is activated by microglial regulation related receptors, including Colony stimulating factor 1 receptor (CSF1R), Fc gamma receptor (FcγR), and TREM2. The Ras has several downstream signaling pathways, including the Raf/ Mek/ Erk (MAPK cascade), phosphatidylinositol-3 kinase (PI3K)-Akt, and Phospholipase C (PLC) signaling pathways. (C) RasV12 mutant is a substitution of G12 with V which disrupts to GTP-GTPase domain of GAPs interaction<sup>43</sup>. Therefore, RasV12 mutant induces constitutive activation of Ras.

### ***Microglial Markers for Immunohistochemistry and Flow Cytometry***

Iba1 and CD11b are widely used as microglial markers but macrophage also express Iba1 and CD11b <sup>44</sup>. A recent study reported that transmembrane protein 119 (Tmem119) is specifically expressed in adult microglia, and its antibody is used for microglia specific marker <sup>45</sup>.

### ***Expression and Function of IL-33 in the CNS***

IL-33 is known to be specifically expressed in Müller glia <sup>46</sup>. Previously, I found that in Glutamine synthetase (GS) expressing Müller glia, IL-33 is specifically expressed in the cell body and pseudopod that localized in the GCL (Fig. 7), suggesting that IL-33 is expressing in the inner retina. IL-33 is reported to change activated microglial phenotypes from neurotoxic to neuroprotective phenotype by upregulating anti-inflammatory factors (IL-10 and TGF- $\beta$ ) in *in vitro* <sup>47</sup>. It is also involved in dendritic spine plasticity via microglial function in the brain <sup>48</sup>. IL-33 receptors consist of the heterodimer: ST2L and IL-1RAcP, which are expressing on microglia, macrophage, mast cells, and regulatory T cells <sup>49</sup>.

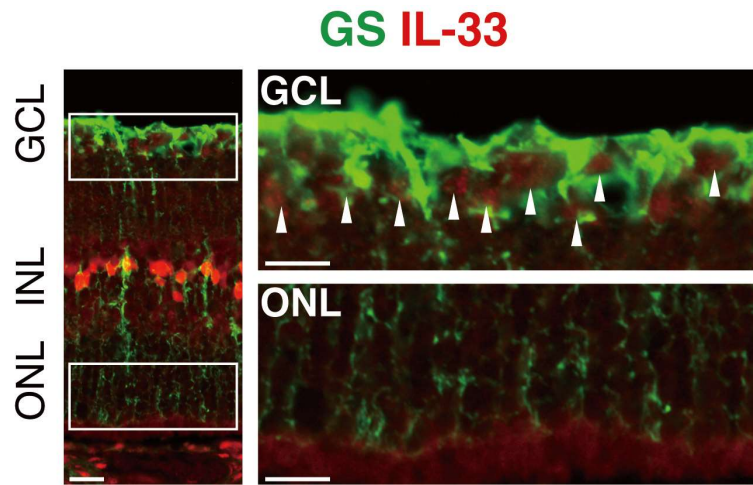


***Figure 7 IL-33 are expressing in Müller glial cell body and pseudopod in the GCL***  
 Glutamine synthetase (GS) (Green) and IL-33 (Red) immunostaining showed that IL-33 were selectively expressing in the Müller glial cell bodies and pseudopods in the GCL (Arrowheads) in adult ICR wild-type mice. Scale bars: 20  $\mu$ m.



***Cx3cr1<sup>tm2.1(cre/ERT2)Jung/J</sup> (Cx3cr1<sup>CreERT2</sup>), pCAG-LSL-EGFP, and pCAG-LSL-RasV12-IRES-EGFP Mice Strain***

Tamoxifen-inducible Cre recombinase (*CreERT2*) is knocked-in into *Cx3cr1* locus in the *Cx3cr1<sup>CreERT2</sup>* mice, and the mice express *CreERT2* under regulation of the *Cx3cr1* promoter<sup>50</sup>. *CreERT2* expresses in tissue-resident macrophages including microglia in *Cx3cr1<sup>CreERT2</sup>* mice<sup>50</sup>.

pCAG-CAT-EGFP mouse carries pCAG-loxP flanked stop codon-EGFP (Fig. 8A)<sup>51</sup>, or *CAG-LSL-RasV12-IRES-EGFP* mouse carries pCAG-loxP flanked stop codon-H-RasV12-IRES-EGFP (Fig. 8B)<sup>52</sup> as the transgenes. These mice lines can induce tissue-specific EGFP or H-RasV12/EGFP expression by crossing with Cre-transgenic mice strain.

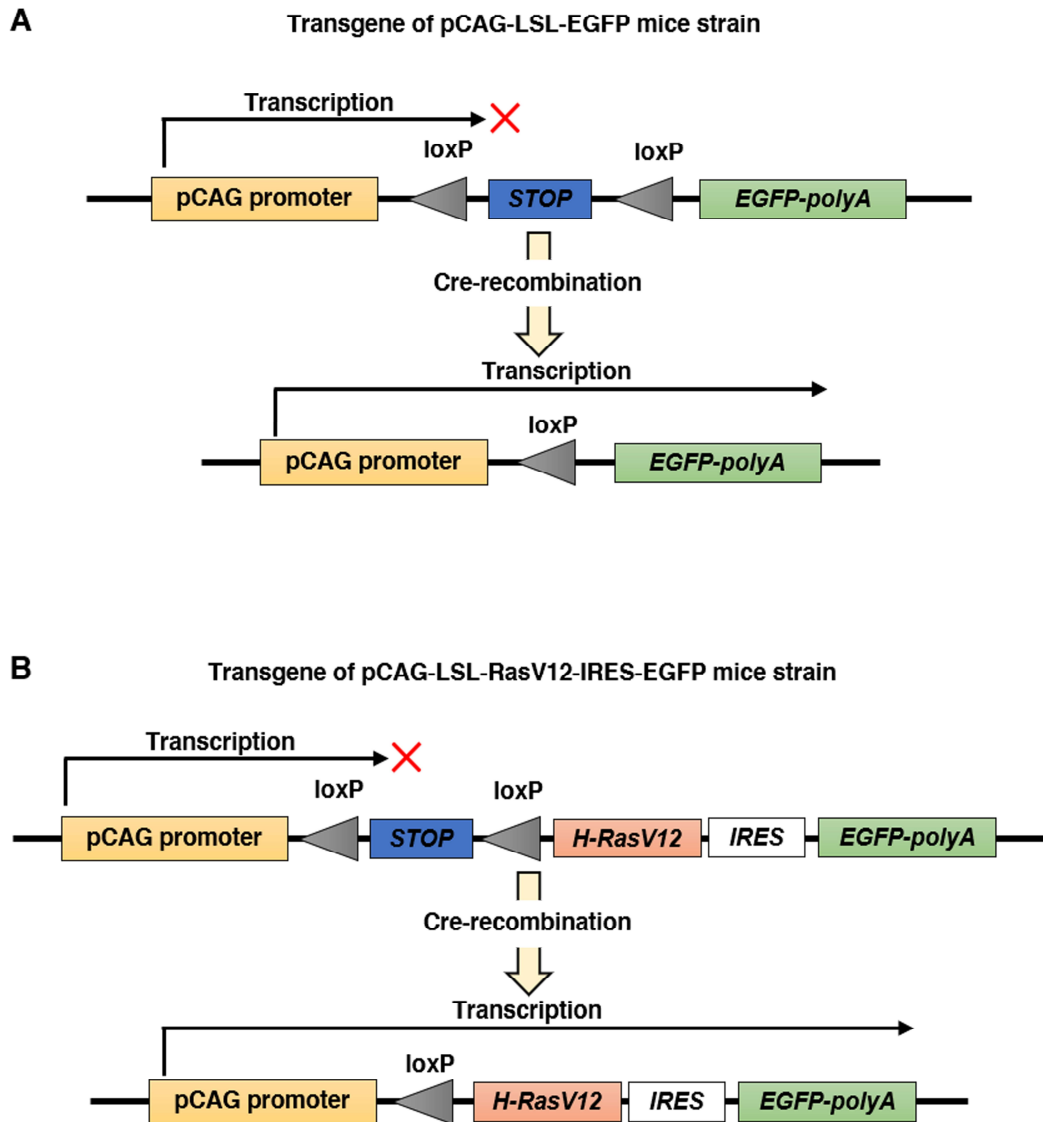


**Figure 8** Transgenes structures of pCAG-LSL-EGFP and pCAG-LSL-RasV12-IRES-EGFP mice

(A) Transgenes structures of pCAG-LSL-EGFP mice strain. The mice have pCAG-loxP flanked stop codon-EGFP as transgene which can express *EGFP* by inducing Cre-recombination. (B) Transgenes structures of pCAG-LSL-RasV12-IRES-EGFP. The mice have pCAG-loxP flanked stop codon- *H-RasV12*-IRES-EGFP as transgene which can express *H-RasV12* and *EGFP* by inducing Cre-recombination.

### ***The Aim of This Study***

This study aimed to investigate the primary effects of activated microglia in the retina using newly established mouse model that carries gene-cassette enabling to express RasV12 in the microglia by exogenous administration of tamoxifen. Previous studies investigated the role of activated microglia in retinal degeneration using retinal degeneration models. By such strategy, it was hard to clarify the role of activated microglia in the early onset of retinal degeneration because there are complex inflammatory circuits in the degenerative retina. Therefore, it is difficult to evaluate contribution of activated microglial during progression of retinal degeneration. Ras is activated by various receptors, that are involved in microglial regulation, such as CSF1 receptor (CSF1R) Fc gamma R (FcγR), and TREM2<sup>2-4</sup>. The expression of H-RasV12 in mouse BV-2 microglial cell line induced upregulation of iNOS and activation of NF-κB signaling pathway, which are responsible for inflammatory cytokines expression<sup>53</sup>. Thus, I chose H-RasV12 in this study to artificially activate microglia. For that purpose, I established mice having transgenes that enable to selectively induce H-RasV12 expression in microglia. I found that H-RasV12 expression in microglia induced microglial proliferation, and H-RasV12 expressed microglia accumulated in the GCL, ONL, and SR, accompanied by photoreceptor-specific degeneration. I also found inducing activation of Müller glial cells, upregulation of photoreceptor injury-related genes: *Edn2* and *Fgf2*, and M1 activated microglia-related genes: *Il1b*, *Il6*, and *Tnf*, suggesting that activation of retinal inflammatory circuits are activated by H-RasV12 expression in microglia.

## Methods

### *Animal Experiments*

All animal experiments were permitted by the Animal Care Committee of the Institute of Medical Science, The University of Tokyo and conducted as required by the ARVO (Association for Research in Vision and Ophthalmology) animal use guidelines.

### *Mice strain, Genotyping, and Tamoxifen Treatment*

C57BL/6J mice were obtained from Japan SLS co. B6.129P2(C)-*Cx3cr1<sup>tm2.1(cre/ERT2)Jung/J</sup>* (*Cx3cr1<sup>CreERT2</sup>*) mice were obtained from Jackson laboratory. To obtain double transgenic mice, *Cx3cr1<sup>CreERT2</sup>* mice<sup>50</sup> were bred with *pCAG-LSL-RasV12-IRES-Egfp* mice<sup>52</sup> or *pCAG-LSL-Egfp* mice<sup>51</sup>. Genotyping of the double transgenic mice: *pCAG-LSL-RasV12-IRES-EGFP*; *Cx3cr1<sup>CreERT2/+</sup>* (*Cx3cr1-RasV12* mice) and *pCAG-LSL-EGFP*; *Cx3cr1<sup>CreERT2/+</sup>* (*Cx3cr1-EGFP*) were conducted by PCR. The sequences of the primers are described in Table 1. The results of the genotyping are described in Table 2. To inducing recombination, fifty µl of tamoxifen (20 mg/mL, dissolved in cone oil, Sigma-Aldrich,) was subcutaneously administrated in the *Cx3cr1-RasV12* mice and *Cx3cr1-EGFP* mice at postnatal day 14. The mice were sacrificed and analyzed at 1, 3, 5, and 7 days post- tamoxifen administration.

### *N-Methyl-N-Nitrosourea (MNU) Treatment for Inducing Photoreceptor Degeneration*

Tamoxifen (0.4 g/kg) was orally administrated in *Cx3cr1<sup>CreERT2/+</sup>* mice and *Cx3cr1-RasV12* mice at 5-weeks-old for 3 days. After 2 days of tamoxifen administration, MNU dissolved in PBS (10 mg/mL, Toronto Research Chemicals) was intraperitoneally administered in mice (30 mg/kg). Mice were sacrificed at 5 days post-MNU administration (7 days post-tamoxifen administration)

### ***IL-33 Treatment for Cx3cr1-RasV12 Mice***

Mouse recombinant mouse IL-33 (0.5 µL) dissolved in PBS (1 µg/mL, PEPRO TECH) was intravitreally administered in the right eye of Cx3cr1-RasV12 mice at 3 days post-tamoxifen administration. As a control, PBS was intravitreally administered in the left eye of Cx3cr1-RasV12 mice or control mice. Mice were sacrificed at 7 days post-tamoxifen administration.

### ***IL-33 and Lipid A Treatment for Mouse MG5 Microglial Cell Line***

Mouse microglial cell line MG5<sup>54</sup> was purchased from JCRB cell bank (IF050520). The cells were maintained in 3:7 mixture of DMEM low glucose (Nacalai tesque) with 10% FBS and A1 (JCRB cell bank, IF050519)-culture conditioned medium. MG5 cells were seeded in 12 well plate ( $1 \times 10^5$  cells) and cultured for overnight at 37 °C. After culturing cells for overnight, the medium was changed from A1-culture conditioned medium to 1 mL of DMEM containing 5 % FBS and Penicillin/ Streptomycin, and MG5 were incubated at 37°C for 1 hour. One µL of Lipid A (diphosphoryl from Salmonella enterica serotype minnesota Re 595, 10 µg/mL, Sigma-Aldrich) and IL-33 (10 µg/mL, PEPRO TECH) were added in MG5 culturing medium. Final concentration of Lipid A and IL-33 was 10 ng/mL). Then, the cells were incubated for 4 hours and collected for RT-qPCR analysis.

### ***Hematoxylin and Eosin (H&E) Staining***

Brain and retina were isolated from the mice after perfusion fixation using 4% paraformaldehyde (PFA)/ PBS and fixed for overnight at 4 °C. The fixed tissues were embedded in paraffin and sectioned (4 µm) using an HM340E microtome (Thermo Scientific Microm). The sections were deparaffinized by Xylene. The deparaffinized sections were stained with Hematoxylin solution (FUJIFILM Wako Pure Chemical) for 10 minutes and washed for 30 minutes by using water. Then, the sections were stained

with Eosin solution (MUTO PURE CHEMICALS). The stained tissues were decolorizing for 20 minutes by ethanol and by xylene for 15 minutes. The H&E stained sections were mounted by Malinol (MUTO PURE CHEMICALS).

### ***Immunohistochemistry (IHC) Analysis***

Immunohistochemistry for frozen retinal sections was conducted as previously described<sup>55</sup>. The brain was isolated from mice after perfusion fixation using 4% PFA/ PBS and fixed for overnight at 4 °C. The tissues were conducted sucrose replacement and sectioned by either 10 or 16 µm thickness using CM1950 cryostat (Leica). Used primary or secondary antibodies are described in Table 3. The sections were stained by the primary antibody for 60 minutes at room temperate and then the primary antibodies were detected by using appropriate fluorescent conjugated secondary antibodies for 60 minutes at room temperate. Imaging was conducted by Axio Imager M1 or M2 microscope (Carl Zeiss). Image editing was conducted by AxioVison ver.4.9.1.0 software (Carl Zeiss). Confocal images were acquired by LSM710 confocal microscope (Carl Zeiss) with ZEN 2009- and ZEN 2.3 lite-software (Carl Zeiss).

### ***Ex Vivo Time-Lapse Imaging by Confocal Microscope***

The retinas of Cx3cr1-RasV12 mice were stained by 0.01 mg/mL of Hoechst33342 (DOJINDO LABORATORIES)/ PBS for 10 minutes at room temperature. Then, The stained retinas were put on Millicell chamber filters (Millipore) and were embedded in 1% agarose (NIPPON GENE)/ PBS at 37 °C. The agarose embedded retinas were conducted time-lapse imaging analysis. The images were acquired 90 times at 1 minute intervals, using LSM710 confocal microscope (Carl Zeiss). Images and movies were edited using ZEN 2009 and ZEN 2.3 lite software (Carl Zeiss).

### ***Flow Cytometric Analysis***

Dissociating of retinal cells from isolated retinas was conducted as previously described<sup>55</sup>. Peripheral blood cells were retrieved from the tail vein of mice. The erythrocytes were eliminated by ACK lysing buffer (Thermo Fisher Scientific). White blood or retinal cells were stained using PE-conjugated anti-CD11b antibody, Alexa Fluor647-conjugated anti-CD73 antibody, or Annexin V-PE. Dead cells were stained with Propidium Iodide (PI). The dilution of antibodies and markers are described in Table 3. Live cells were gated and were analyzed by FACS Calibur (BD Biosciences). Data analysis was conducted by Flow Jo software (BD Biosciences).

### ***Reverse Transcription and Quantitative PCR (RT-qPCR)***

Total RNA was extracted from mouse whole retina and MG5 using Sepasol RNA I Super G (Nacalai Tesque), and cDNA was synthesized by ReverTra Ace qPCR RT Master Mix (TOYOBO). Quantitative PCR (qPCR) was conducted using the THUNDERBIRD SYBR qPCR Mix (TOYOBO). The qPCR and measuring fluorescent were conducted using Roche Light Cycler 96 (Roche Diagnostics). *Actb* and *Sdha* gene expression levels were used as reference genes for endogenous control.

### ***Statistical Analysis***

All statistical analysis was conducted by R software (The R Foundation for Statistical Computing). p values were computed by Wilcoxon rank-sum test (also known as Mann-Whitney U test) using R package 'exactRankTests' or One-way ANOVA Tukey-Kramer test using R command 'TukeyHSD'. Data presented as mean with SEM.

**Table 1 The Primer Sequences for Genotyping**

Primer names	Sequences (5' to 3')
Cre-Forward	TCT AGC GTT CGA ACG CAC TGA
Cre-Reverse	CAC CAT TTT TTC TGA CCC G
pCAG-LSL-EGFP-Forward	CAG TCA GTT GCA CAA T
pCAG-LSL-EGFP-Reverse	ATA TCA CCA GCT CAC CGT CTT
pCAG-LSL-RasV12-EGFP-Forward	CAC TGT GGA ATC TCG GCA GG
pCAG-LSL-RasV12-EGFP-Reverse	GCA ATA TGG TG AAA ATA AC

**Table 2 Genotyping Results of Transgenic Mice**

Cx3cr1-EGFP genotypes (n=107)	Expected No.(%)	Observed No.(%)
<i>Cre</i> /+; +/+	54 (50%)	61 (57%)
<i>Cre</i> /+; <i>EGFP</i> /+	54 (50%)	46 (43%)
Cx3cr1-RasV12 genotypes (n=214)	Expected No.(%)	Observed No.(%)
<i>Cre</i> /+; +/+	107 (50%)	118 (55%)
<i>Cre</i> /+; <i>RasV12</i> /+	107 (50%)	96 (45%)



**Table 3 Antibodies and Makers Information for IHC and Flow Cytometry Analysis**

Species	Antibody names	Dilution	Maker names
<i>Primary antibodies for IHC analysis</i>			
Mouse	Anti-Ap-2 $\alpha$	1:50	DSHB
Goat	Anti-Brn3b	1:100	Santa Cruz Biotechnology
Rabbit	Anti-Calbindin	1:500	EMD Millipore
Rat	Anti-CD68	1:2000	BIO-RAD
Sheep	Anti-Chx10	1:500	Exalpha Biological Inc
Mouse	Anti-GFAP	1:400	Sigma-Aldrich
Chicken	Anti-GFP	1:2000	Abcam
Rabbit	Anti-Iba1	1:1000	FUJIFILM Wako Pure Chemical
Mouse	Anti-iNOS	1:500	Novus
Mouse	Anti-Ki67	1:100	BD Pharmingen
Rabbit	Anti-NeuN	1:1000	Abcam
Mouse	Anti-pMAPK (pErk1/2)	1:2000	Cell Signaling Technology
Rabbit	Anti-RBPMS	1:2000	Abcam
Rabbit	Anti-Recoverin	1:1000	Abcam
Mouse	Anti-Rhodopsin	1:200	LSL
Rabbit	Anti-Tmem119	1:250	Abcam
<i>Secondary antibody for IHC analysis</i>			
Goat	Alexa Fluor® 488 goat Anti-chicken IgG(H+L)	1:250	Thermo Fisher Scientific
Goat	Alexa Fluor® 568 goat Anti-mouse IgG(H+L)	1:250	Thermo Fisher Scientific
Goat	Alexa Fluor® 568 goat Anti-rabbit IgG(H+L)	1:250	Thermo Fisher Scientific
Goat	Alexa Fluor® 594 goat Anti-mouse IgG(H+L)	1:250	Thermo Fisher Scientific
Goat	Alexa Fluor® 594 goat Anti-rabbit IgG(H+L)	1:250	Thermo Fisher Scientific

Goat	Alexa Fluor® 680 goat Anti-mouse IgG(H+L)	1:250	Thermo Fisher Scientific
Goat	Alexa Fluor® 680 goat Anti-rabbit IgG(H+L)	1:250	Thermo Fisher Scientific
<i>Antibodies or markers for flow cytometry analysis</i>			
Rat	Alexa Fluor647-conjugated anti-CD73 antibody	1:100	BD Biosciences
Rat	PE-conjugated anti-CD11b antibody	1:100	Bio Legend
N/A	PE-conjugated Annexin V	1:100	Bio Vison
N/A	Propidium Iodide	1:1000	Sigma-Aldrich

Antibodies and markers are diluted by 2% BSA/PBS as indicated in Table 3.

## Results

### ***Generation of Microglial Activation Model by Selectively Expressing H-RasV12 in Microglia***

In this study, I used the double transgenic mice lines *CAG-LSL-H-RasV12-IRES-EGFP*; *Cx3cr1<sup>CreERT2/+</sup>* and *CAG-LSL-EGFP*; *Cx3cr1<sup>CreERT2/+</sup>*. The double transgenic mice lines are denoted as Cx3cr1-RasV12 and Cx3cr1-EGFP mice respectively. The chemokine receptor CX3CR1 had been reported to be dominantly expressed in the monocytes, macrophages, and tissue-resident macrophages including microglia<sup>56</sup>. The Cx3cr1-RasV12 and Cx3cr1-EGFP mice expressing tamoxifen-inducible Cre recombinase in microglia. Thus, Cx3cr1-RasV12 mice or Cx3cr1-EGFP mice can induce expression of RasV12-EGFP or EGFP in microglia by tamoxifen administration. I first confirmed whether pups of Cx3cr1-EGFP (as used for control) and Cx3cr1-RasV12 mice were born with Mendelian ratio. The pups were born with a predicted Mendelian ratio approximately (Table 2).

Tamoxifen was administrated into Cx3cr1-EGFP and Cx3cr1-RasV12 mice by subcutaneous administration at postnatal day 14. Cx3cr1-RasV12 mice were dead at 8-10 days after tamoxifen administration. Because *Cx3cr1* is also expressing monocytes in peripheral blood<sup>56, 57</sup>, I confirmed the expression of EGFP or RasV12-EGFP in monocytes in the Cx3cr1-EGFP or Cx3cr1-RasV12 mice by flow cytometry analysis (Fig. 9A). Monocytes and microglia are detected by, a microglia/ monocytes/ macrophage-specific marker, CD11b. In both Cx3cr1-EGFP and Cx3cr1-RasV12 mice, about 2% of CD11b-positive monocytes expressed EGFP (Fig. 9A, B), suggesting that few monocytes expressed RasV12-EGFP in the peripheral blood, and leukemia-like phenotypes such as the abnormal proliferation of monocytes were not detected in the Cx3cr1-RasV12 mice. In the retina, 50% of CD11b-positive microglia/macrophages expressed EGFP in both Cx3cr1-EGFP and Cx3cr1-RasV12 mice (Fig. 9A, B).

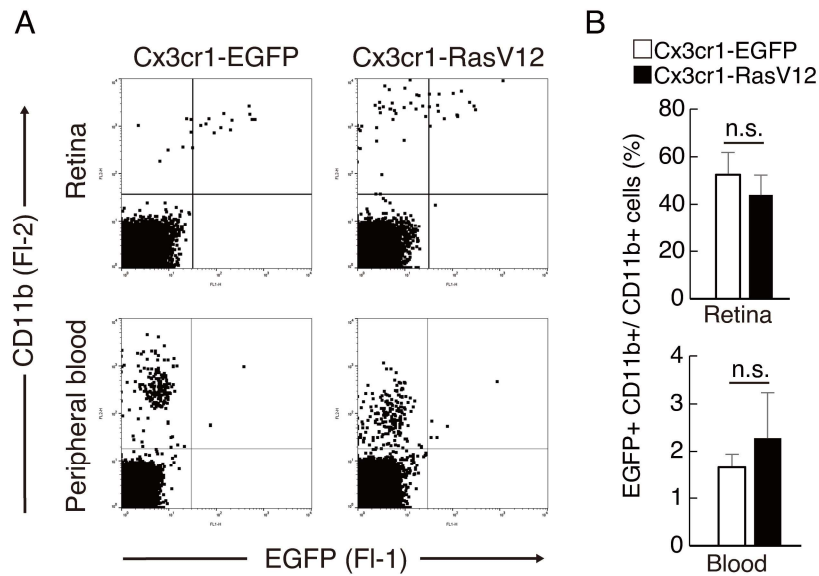


**Figure 9 Expression patterns of EGFP and CD11b in the peripheral blood and retina in the Cx3cr1-EGFP or Cx3cr1-RasV12 mice**

(A) White blood cells and retinal cells were collected using the same mouse, and monocytes or microglia were detected using PE-conjugated anti-CD11b antibody. (B) The population of EGFP and CD11b double-positive cells in the total CD11b positive cells. about 50% of CD11b positive microglia also expressed EGFP in the retinas, whereas about 2% of CD11b positive monocytes/ macrophages also expressed EGFP in the peripheral blood.

Data presented as mean with SEM. (n=6 per group, Mann-Whitney U test, n.s. not significant).

Cx3cr1 is involved in suppressing of microglial activation. I checked the microglial number and distribution in the retinas of Cx3cr1-EGFP mice because in the Cx3cr1-EGFP mice, one of the Cx3cr1 alleles was replaced with the *CreERT2* encoding DNA sequence. Flow cytometry analysis showed that about 1% of CD11b-positive microglia were detected in both retinas of wild-type and Cx3cr1-EGFP (Fig. 10A). Immunohistochemistry analysis showed that Iba1-positive microglia were in the IPL and INL, and the number and distribution of Iba1-positive microglia were not significantly different between wild-type and Cx3cr1-EGFP mice (Fig. 10B).



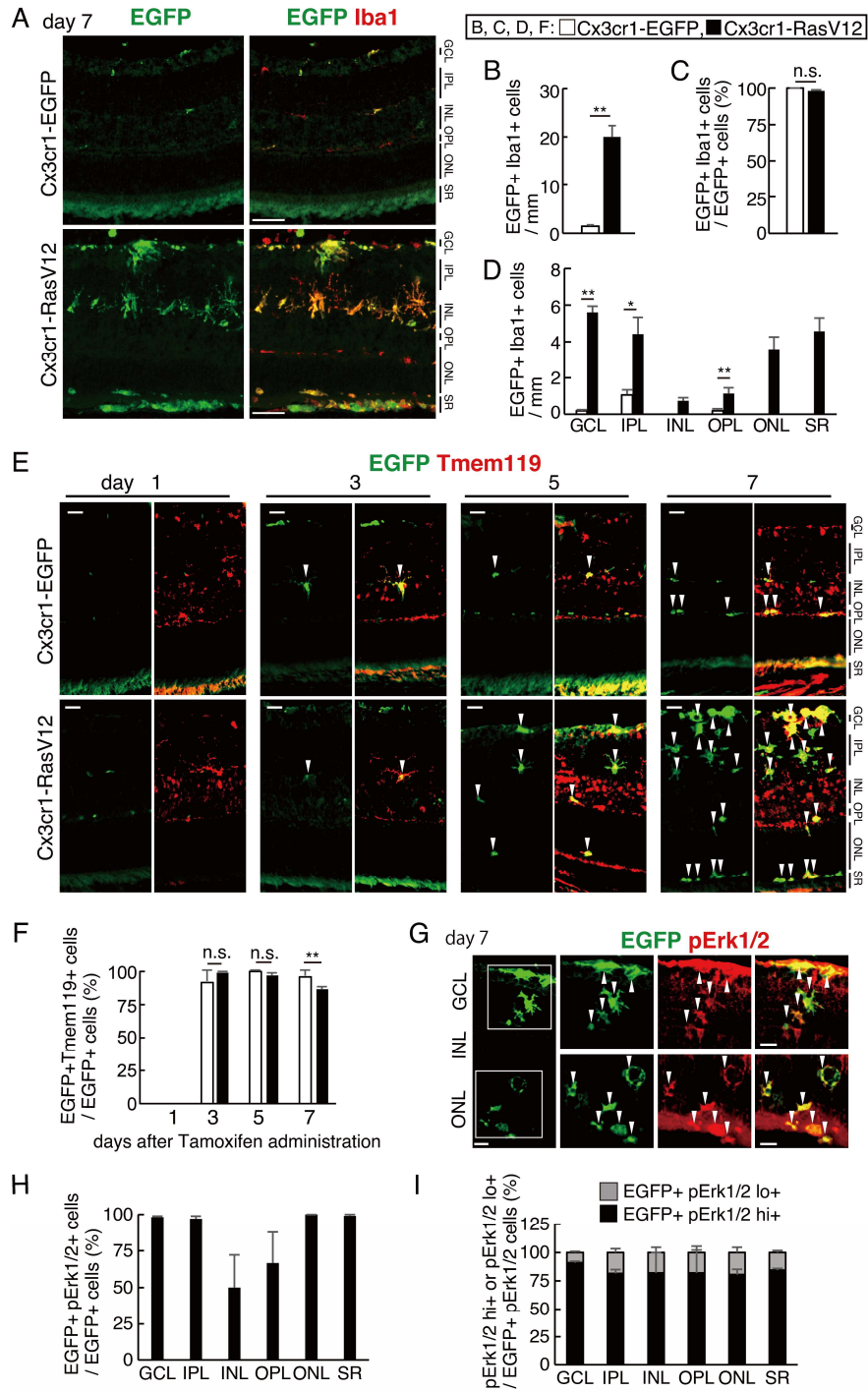
Data presented as mean with SEM. (n=3 per group, Mann-Whitney U test., n.s. not significant). Scale bars: (B), 20  $\mu$ m

GCL; ganglion cell layer. IPL; inner plexiform layer. OPL; outer plexiform layer. ONL; outer nuclear layer. Total; the total cell number of positive cells.

### ***Retinal and Brain Phenotypes of Ras-Expressing Microglia***

To confirm the distribution of RasV12-expressing microglia in the retina and the brain, mice were sacrificed at 7 days after tamoxifen administration and analyzed by immunohistochemistry analysis. The number of EGFP positive cells significantly increased in the Cx3cr1-RasV12 mice compared to Cx3cr1-EGFP mice (Fig. 11A, B). Moreover, more than 90% of EGFP positive cells also expressed, microglia and macrophage marker, Iba1 in both Cx3cr1-EGFP and Cx3cr1-RasV12 mice retina (Fig. 11C). Ramified microglia localized in the IPL and OPL <sup>58</sup>. EGFP and Iba1 double-positive cells existed in IPL and OPL in the Cx3cr1-EGFP mice, whereas the cells accumulated in the GCL, IPL, INL, and SR of Cx3cr1-RasV12 mice at 7 days post-tamoxifen administration (Fig. 11D), indicating that Rasv12-expressing microglia migrated to the GCL and SR. Next, I conducted time-course analysis of EGFP expression at 1, 3, 5, and 7 days post- tamoxifen administration. Expression of EGFP was observed from 3 days post- tamoxifen administration in retinas of Cx3cr1-EGFP and Cx3cr1-RasV12 mice (Fig. 11E, arrowheads). EGFP-positive cells also expressed, a microglia-specific marker, Tmem119 (Fig. 11E) <sup>45</sup>. More than 90% of EGFP positive cells also expressed Tmem119 in both Cx3cr1-EGFP and Cx3cr1-RasV12 mice retina at 3, 5, and 7 days post-tamoxifen administration (Fig. 11F). Furthermore, immunostaining of phosphorylated ERK1/2 (pErk1/2) and EGFP showed that all of Erk1/2 was phosphorylated in RasV12-EGFP-positive cells (Fig. 11G arrowheads), suggesting that the Ras-MAPK signaling pathway were activated in the RasV12-EGFP-positive microglia. The population of EGFP and pErk1/2 double-positive cells in the total EGFP-positive cells was not different between the inner and outer sides of the retina in the Cx3cr1-RasV12 (Fig. 11H). The EGFP-positive cells have strong or weak pErk1/2 signals. However, the ratio of weak pErk1/2-positive cells or strong pErk1/2-positive cells in EGFP-positive cells was not different in all retinal regions (Fig. 11I).





ONL, and SR in Cx3cr1-RasV12 mice **(B)** The total number of EGFP and Iba1 double-positive cells at 7 days post-tamoxifen administration in the retina. **(C)** The population of EGFP and Iba1 double-positive cells in total EGFP-positive cells in the retina **(D)** The number of EGFP and Iba1-double positive cells was counted in each retinal layer. **(E)** EGFP (Green) and Tmem119 (Red) immunostained retinas at 1, 3, 5, and 7 days post-tamoxifen administration. White arrowheads indicate EGFP and Tmem119 double-positive cells. **(F)** The populations of EGFP and Tmem119-double positive cells in total EGFP positive cells in the retina. **(G)** EGFP (Green) and phosphorylated Erk1/2 (pErk1/2) (Red) immunostained retinal sections at 7 days post-tamoxifen administration. The EGFP-positive cells have strong or weak pErk1/2 signals. White arrowheads indicate EGFP and pErk1/2 double-positive cells. **(H)** The population of EGFP and pErk1/2-double positive cells in the total EGFP positive cells in each retinal layer. **(I)** The ratio of weak pErk1/2-positive cells or strong pErk1/2-positive cells in EGFP-positive cells in each retinal layer.

Scale bars: (A), 50  $\mu\text{m}$ ., (E, G), 20  $\mu\text{m}$ . Data presented as mean with SEM. Asterisks indicate significant differences (n=6 per group, Mann-Whitney U test., \*  $p<0.05$ , \*\*  $p<0.01$ , n.s., not significant).

GCL; ganglion cell layer. IPL; inner plexiform layer. INL; inner nuclear layer. OPL; outer plexiform layer. ONL; outer nuclear layer. SR; subretinal regions

I then analyzed the brain of Cx3cr1-RasV12 mice. Microglia were also found in the brain<sup>59</sup>, and these microglia express Cx3cr1<sup>50</sup>. Therefore, I analyzed the brain as a typical example of the CNS that is likely existing RasV12-expressing microglia. In the brain, the increased-number of EGFP-positive cells was observed in the ventral orbital cortex (VO), lateral orbital cortex (LO), and ventral tenia tecta (VTT) at day 7 days post-tamoxifen administration in Cx3cr1-RasV12 mice (Fig. 12A). Hematoxylin and Eosin staining revealed that strong Eosin staining but neurodegenerative regions were not observed in the VO, LO, and VTT in the Cx3cr1-RasV12 mice (Fig. 12B). To examine degenerative conditions in the Cx3cr1-RasV12 mice, brains were immunostained with, a pan-neuron marker, NeuN. Morphology and the number of NeuN-positive cells was indistinguishable between Cx3cr1-EGFP and Cx3cr1-RasV12 mice in the brain (Fig. 12C, D), suggesting that degenerative neurons were not detected in the brain of Cx3cr1-RasV12 mice. Also, Cx3cr1-RasV12 mice did not show other pathological phenotypes (e.g. cancerogenesis, a deposit of abnormal proteins, and necrosis), supporting the idea that the brain was not severely damaged.

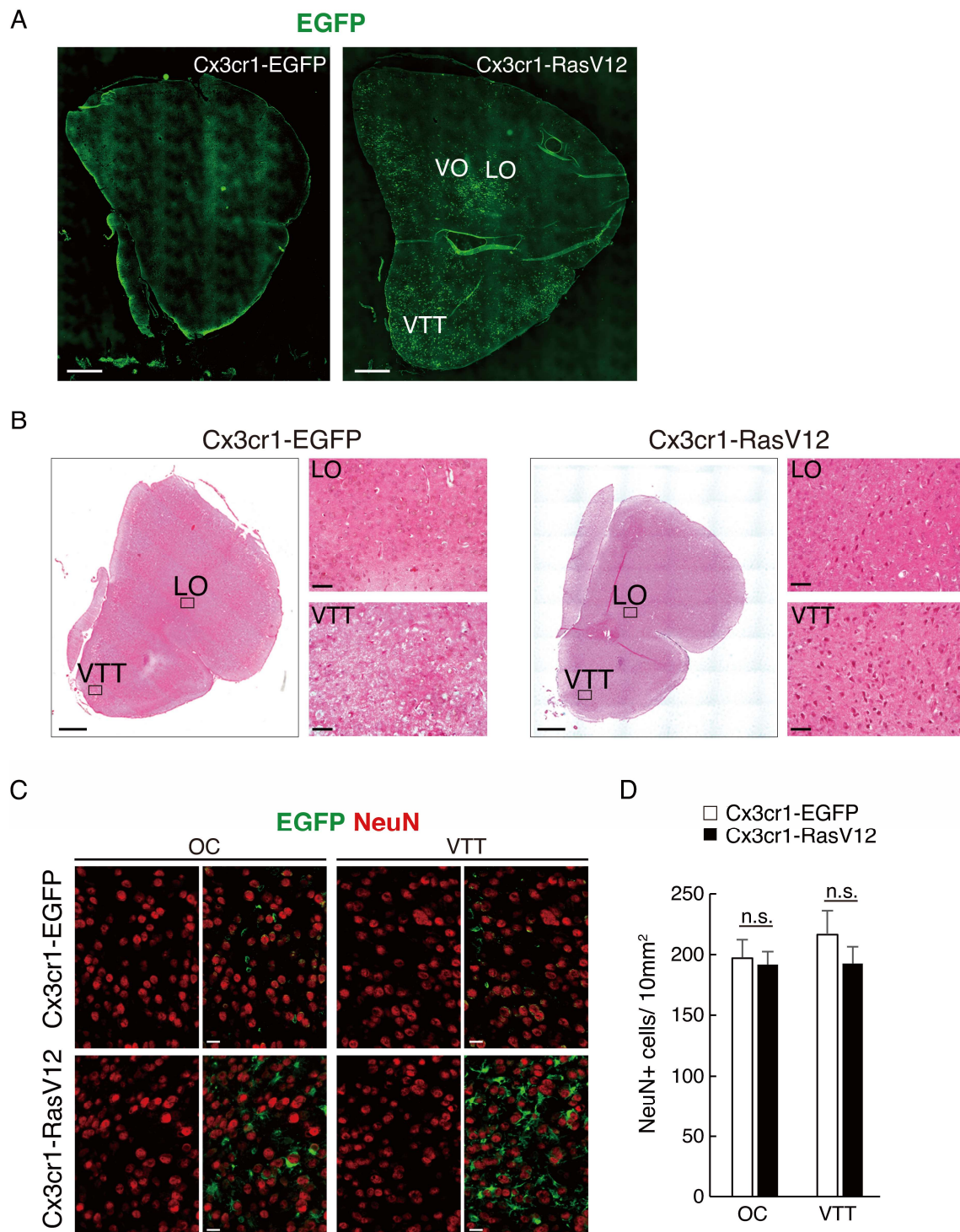


**Figure 12 Histological analysis of the brain in Cx3cr1-RasV12 mice**

(A) EGFP (Green) immunostained brain sections of Cx3cr1-EGFP and Cx3cr1-RasV12 mice at 7 days post-tamoxifen administration. (B) Hematoxylin and Eosin stained brains of Cx3cr1-EGFP and Cx3cr1-RasV12 mice at 7 days post-tamoxifen administration.

Neurodegenerative regions were not detected in the Cx3cr1-RasV12 mice. **(C)** EGFP (Green) and NeuN (Red) immunostained brain sections of Cx3cr1-EGFP and Cx3cr1-RasV12 mice at 7 days post-tamoxifen administration. Morphology and the number of NeuN-positive cells did not change between control and Cx3cr1-RasV12 mice. **(D)** The number of NeuN-positive cells in the orbital cortex.

Scale bars: (A, Whole section panels of B), 200  $\mu\text{m}$ ., (Enlarged panels of B, C), 50  $\mu\text{m}$ . Data presented as mean with SEM. Asterisks indicate significant differences (n=4 per group, Mann-Whitney U test., n.s., not significant).

VO; ventral orbital cortex. LO; lateral orbital cortex. VTT; ventral tenia tecta.

The expression of EGFP was observed from 3 days post-tamoxifen administration as well as the retina (Fig. 13A) and also the EGFP and Iba1 double-positive cells were detected in the orbital cortex region (Fig. 13A arrowheads). More than 90% of EGFP-positive cells expressed Iba1 in total EGFP-positive cells in the Cx3cr1-EGFP and Cx3cr1-RasV12 mice at 7 days post-tamoxifen administration (Fig. 13B). The number of EGFP and Iba1 double-positive cells significantly increased from 5 days post-tamoxifen administration in the brain of Cx3cr1-RasV12 mice compared to Cx3cr1-EGFP mice (Fig. 13C). Furthermore, phosphorylation of Erk1/2 was detected in EGFP-positive cells in the orbital cortex region of Cx3cr1-RasV12 mice as well as retinas (Fig. 13D, arrowheads).

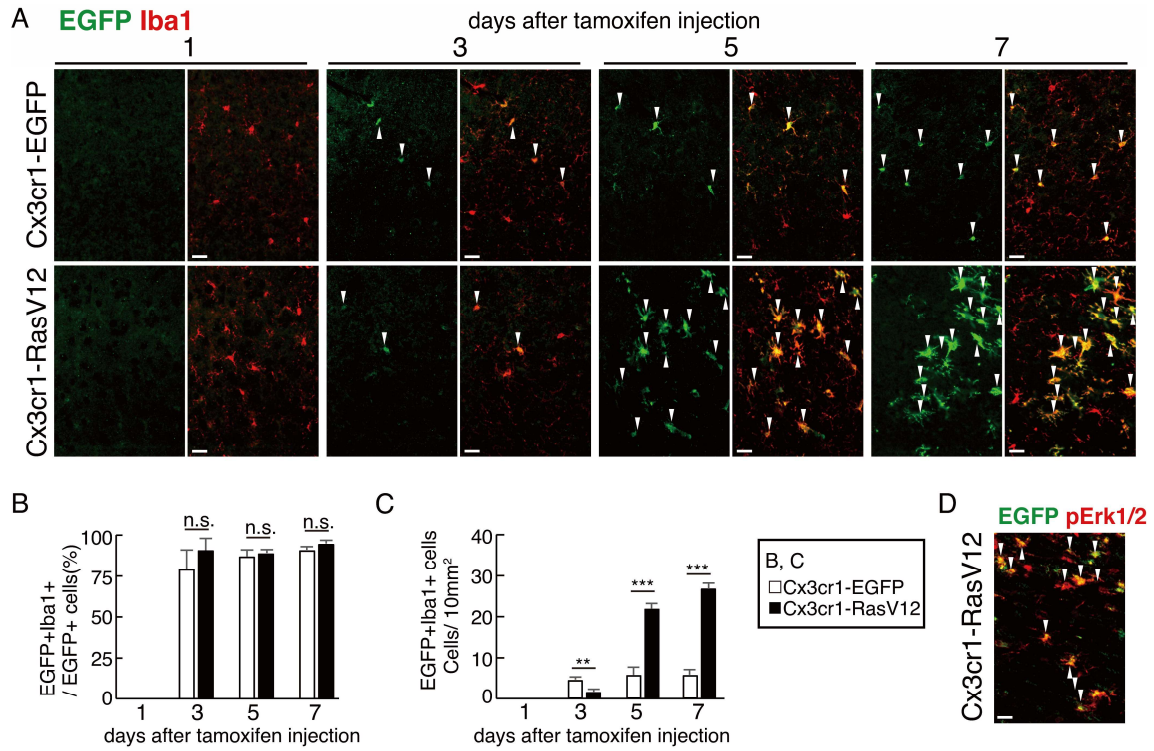


**Figure 13 Expression of RasV12-EGFP and phosphorylation of Erk1/2 in the microglia in Cx3cr1-RasV12 mice**

(A) EGFP (Green) and Iba1 (Red) immunostained brain sections at 7 days post-tamoxifen administration in the orbital cortex regions. EGFP and Iba1 double-positive cells were indicated by white arrowheads. (B) The population of EGFP and Iba1-double positive cells in total EGFP positive cells in the orbital cortex regions. (C) The number of EGFP and Iba1-double positive cells in the orbital cortex regions. (D) EGFP (Green) and phosphorylated Erk1/2 (pErk1/2) (Red) immunostained brain sections of Cx3cr1-RasV12 mice at 7 days post-tamoxifen administration in the orbital cortex regions. White arrowheads indicate EGFP and pErk1/2 double-positive cells.

Scale bars: (A, D), 20  $\mu$ m. Data presented as mean with SEM. Asterisks indicate significant differences (n=4 per group, Mann-Whitney U test., \*\*  $p < 0.01$ , \*\*\*  $p < 0.001$ , n.s., not significant).

### ***Distribution and Proliferation of Retinal RasV12-Expressing Microglia, and Cytokines Expression in the Cx3cr1-RasV12 Mice***

In this part, I focused on the retinal phenotypes of RasV12-expressing microglia and analyzed the Cx3cr1-RasV12 mice. The number of EGFP and Tmem119-double positive cells increased from 5 to 7 days post-tamoxifen administration in Cx3cr1-RasV12 retinas (Fig. 14A, B). The Cx3cr1-RasV12 mice significantly increased the number of EGFP and Tmem119-double positive cells compared to Cx3cr1-EGFP retinas at 7 days post-tamoxifen administration (Fig. 14A, B). Furthermore, RasV12-EGFP positive cells also expressed, a proliferation marker, Ki67 in the Cx3cr1-RasV12 mice, whereas EGFP and Ki67-double positive cells were not detected in the Cx3cr1-EGFP mice (Fig. 14C, arrowheads). More than 70% of EGFP-positive cells expressed Ki67 in total EGFP-positive cells in the Cx3cr1-RasV12 mice at 7 days post-tamoxifen administration (Fig. 14D). EGFP and Ki67-double positive cells were detected in all retinal layers (Fig. 14E). RasV12-EGFP-positive cells showed ameboid-like morphology (Fig. 14C), which is one of the typical features of microglial activation<sup>29,59</sup>. Another feature of activated microglia is the upregulation of chemokines and inflammatory cytokines<sup>27,61</sup>. The Cx3cr1-RasV12 mice were significantly upregulated *Ccl2*, *Ccl3*, *Cxcl1*, *Cxcl5*, *Il1b*, *Il6*, and *Tnf* expression compared to the Cx3cr1-EGFP mice in the retina (Fig. 14F).



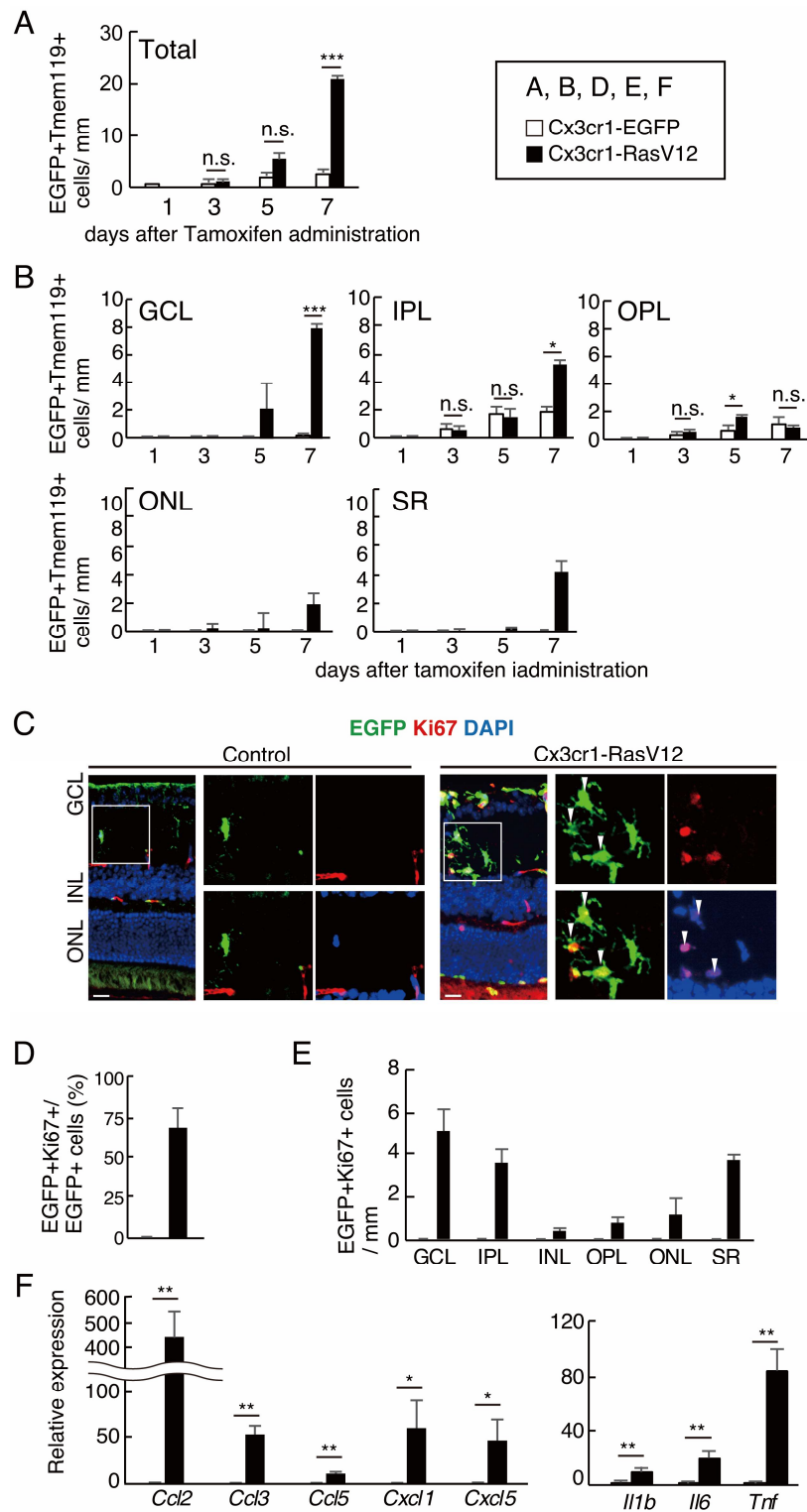


**Figure 14** Distribution of retinal RasV12-expressing microglia and activated microglia phenotypes in the Cx3cr1-RasV12 mice

**(A)** The total number of EGFP and Tmem119-double positive cells in the retinas of the Cx3cr1-EGFP and Cx3cr1-RasV12 mice at 1, 3, 5, and 7 days post-tamoxifen administration. Immunohistochemistry images are shown in Figure. 11E. **(B)** The distribution of RasV12-EGFP or EGFP expressing-microglia in the retinas of the Cx3cr1-EGFP and Cx3cr1-RasV12 mice at 1, 3, 5, and 7 days post-tamoxifen administration. The number of EGFP and Tmem119-double positive cells were respectively counted in the GCL, IPL, ONL, and SR. **(C-E)** Results for EGFP and Ki67 immunostaining of retina. **(C)** EGFP (Green) and Ki67 (Red) immunostained retinal sections at 7 days post-tamoxifen administration. EGFP and Ki67 double-positive cells were indicated by white arrowheads **(D)** The population of EGFP and Ki67 double positive cells in total EGFP positive cells. **(E)** The number of EGFP and Ki67-double positive cells in each retinal layer **(F)** Gene expression patterns of chemokines and cytokines in the retina at 7 days post-tamoxifen administration, in which are a marker for activated microglia. Gene expressions were quantified by RT-qPCR.

Scale bars: (C), 20  $\mu$ m. Data presented as mean with SEM. Asterisks indicate significant differences (n=6 per group, Mann-Whitney U test., \*  $p < 0.05$ , \*\*  $p < 0.01$ , \*\*\*  $p < 0.001$ , n.s., not significant).

GCL; ganglion cell layer. IPL; inner plexiform layer. INL; inner nuclear layer. OPL; outer plexiform layer. ONL; outer nuclear layer. SR; subretinal regions. Total; the total cell number of positive cells.

In the brain of Cx3cr1-RasV12 mice at 7 days post-tamoxifen administration, EGFP and Ki67-double positive cells were detected in the orbital cortex as well as retinas (Fig. 15A, B). Although less than 30% of EGFP-positive cells only expressed Ki67 in total EGFP-positive cells (Fig. 15C).

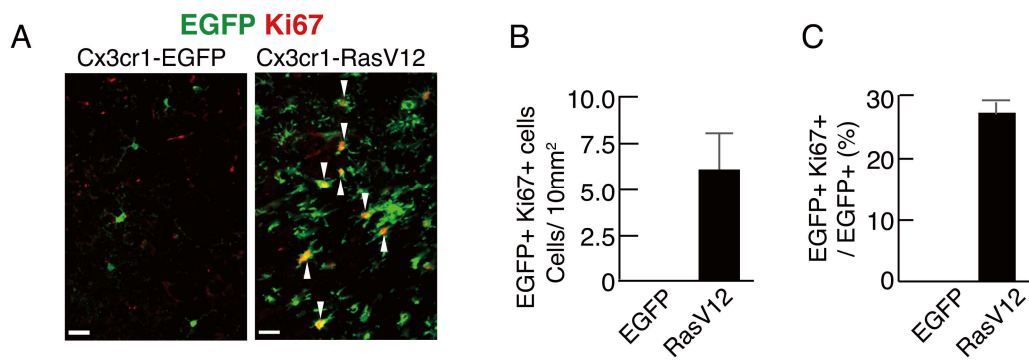


**Figure 15 RasV12 expressing microglia had proliferation activity in the brain**

(A) EGFP (Green) and Ki67 (Red) immunostained brain sections at 7 days post-tamoxifen administration in the orbital cortex regions. EGFP and Ki67-double positive cells were indicated by white arrowheads. (B) The number of EGFP and Ki67-double positive cells in the orbital cortex regions. (C) The population of EGFP and Ki67-double positive cells in the total EGFP positive cells in the orbital cortex regions.

Scale bars: (A), 20  $\mu$ m. Data presented as mean with SEM (n=4 per group)

### ***RasV12-Expressing Microglia Induced Photoreceptor-Specific Degeneration***

To confirm retinal tissue phenotypes of the Cx3cr1-RasV12 mice, H&E staining was conducted. The lack of ONL nucleus was observed in Cx3cr1-RasV12 mice (Fig. 16A, arrowheads in the enlarged picture). Furthermore, the reduction of Rhodopsin-positive regions, a rod photoreceptor outer segments, was observed in the Cx3cr1-RasV12 mice (Fig. 16B). Consistently, the thickness of the outer segments was significantly thinned in the Cx3cr1-RasV12 mice compared to Cx3cr1-EGFP mice (Fig. 16B, C). Also, the Cx3cr1-RasV12 mice showed that EGFP-positive cells accumulated in the ONL-SR and had Rhodopsin-positive regions in the cell body (Fig. 16B), suggesting that RasV12-expressing microglia phagocytosed photoreceptors. Next, I checked the exposure of phosphatidylserine (PS) on rod photoreceptors to confirming the photoreceptor's condition. Exposure of PS on the outer side of the cell membrane acts as an eat-me signal on injured photoreceptor <sup>62</sup>. I used Annexin V and anti-CD73 antibodies as markers for PS and rod photoreceptor cells respectively. CD73 is a specific marker for matured rod photoreceptors in the adult retina (also known as a marker for photoreceptor precursor cells in the developing retina) <sup>63</sup>. Also, Propidium Iodide (PI), a dead cell maker, -positive and Annexin V-positive cells are known as apoptotic cells <sup>64</sup>. Cx3cr1-RasV12 mice showed that Annexin V-positive cells were only detected in CD73-positive fraction of Cx3cr1-RasV12 mice (Fig16. D), and the population of Annexin V-positive and PI-negative cells significantly higher in CD73-positive fraction in Cx3cr1-RasV12 mice (Fig. 16E).

Retinal degeneration is characterized by Müller glial activation <sup>39</sup> and upregulation of Edn2 and FGF2 in the photoreceptors <sup>37, 40</sup>. The retinas of Cx3cr1-RasV12 mice upregulated expression of *Edn2* and *Fgf2* (Fig. 16F) and, an activated Müller glial marker, glial fibrillary acidic protein (GFAP). <sup>65</sup> (Fig. 16G, H).

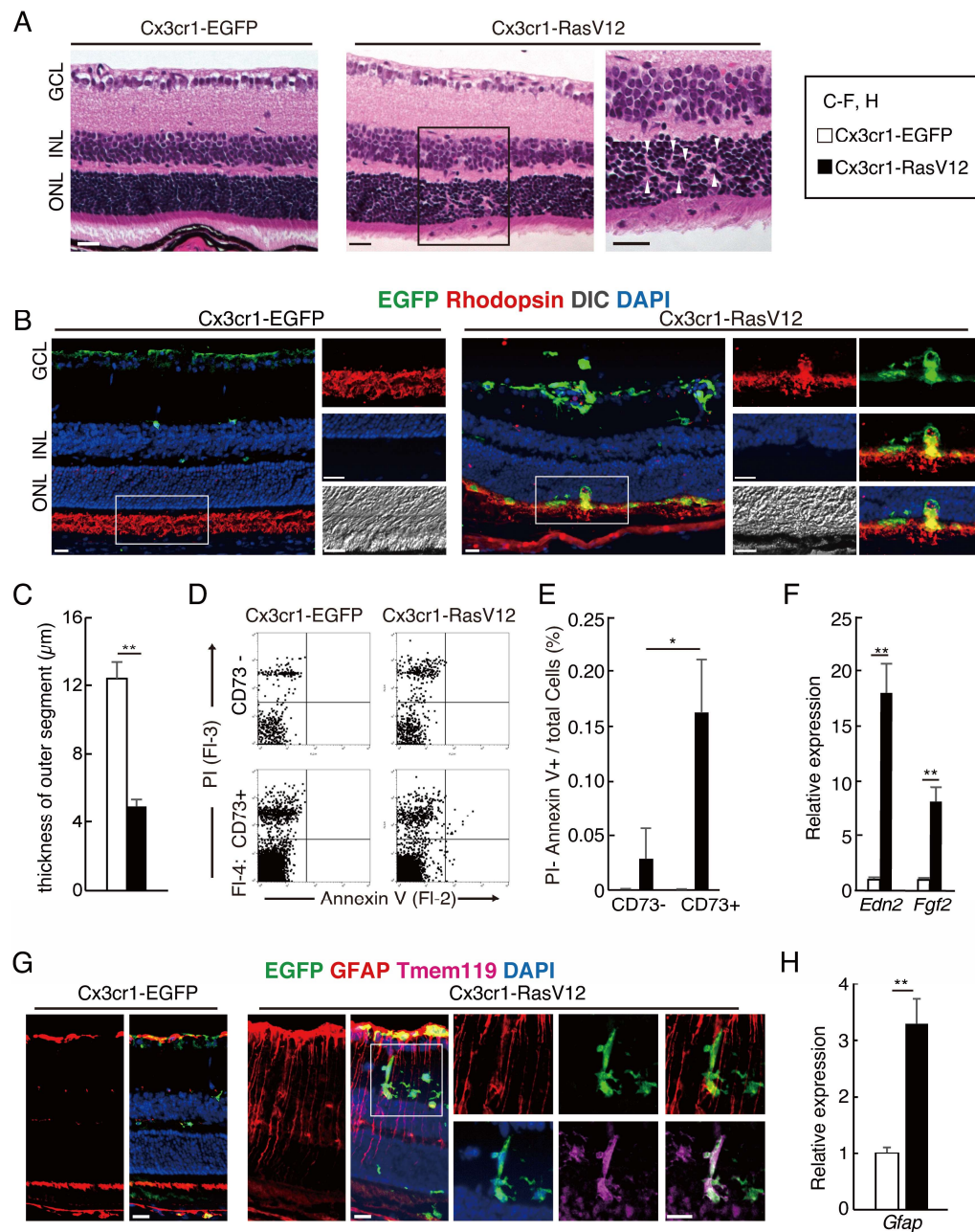


**Figure 16 Induction of photoreceptor degeneration and Müller glial activation in the *Cx3cr1-RasV12* mice**

(A) Hematoxylin and Eosin stained retinal sections of *Cx3cr1-EGFP* or *Cx3cr1-RasV12* mice at 7 days post-tamoxifen administration. White arrowheads indicate a lack of photoreceptor nuclei regions in the ONL. (B) EGFP (Green) and Rhodopsin (Red) stained sections of *Cx3cr1-EGFP* or *Cx3cr1-RasV12* mice at 7 days post-tamoxifen

administration. Also, showing differential interference contrast (DIC) images. **(C)** Quantification of outer-segment thickness of Cx3cr1-EGFP or Cx3cr1-RasV12 mice. The thickness was measured from DIC images in Fig. 16B **(D, E)** Flow cytometrical analysis of retinas in the Cx3cr1-EGFP or Cx3cr1-RasV12 mice at 7 days post-tamoxifen administration. Rod photoreceptors, phosphatidylserine (PS) exposing cells, dead cells were labeled using Alexa Fluor647-conjugated anti-CD73 antibody, PE-conjugated Annexin V, and Propidium Iodide (PI) respectively. Upper panels indicate CD73-negative cell fractions, whereas lower panels indicate CD73-positive cell fractions.

**(E)** The population of PI-negative and Annexin V-positive cells in CD73-negative or CD73-positive cell fractions. **(F)** Gene expression patterns of photoreceptor degeneration-related genes in Cx3cr1-EGFP or Cx3cr1-RasV12 mice at 7 days post-tamoxifen administration. Gene expression levels were quantified by RT-qPCR. **(G)** EGFP (Green), GFAP (Red), and Tmem119 (Magenta) stained sections of Cx3cr1-EGFP or Cx3cr1-Ras mice at 7 days post-tamoxifen administration. **(H)** Gene expression level of *Gfap* in Cx3cr1-EGFP or Cx3cr1-RasV12 mice at 7 days post-tamoxifen administration. The gene expressions were quantified by RT-qPCR.

Scale bars: (A, B, G), 20  $\mu$ m. Data presented as mean with SEM. Asterisks indicate significant differences (n=4 ~6 per group, Mann-Whitney U test., \*p< 0.05, \*\* p< 0.01). DIC; differential interference contrast. PI; Propidium Iodide PS; phosphatidylserine

I next confirmed whether degenerations can be observed in other retinal cells of Cx3cr1-RasV12 mice or not. There are no significant differences in morphology and numbers of RBPMS-positive retinal ganglion cells (Fig. 17A), AP-2 $\alpha$ -positive amacrine cells (Fig. 17B), Chx10-positive bipolar cells (Fig. 17C), and Calbindin-positive horizontal cells (Fig. 17D) between the Cx3cr1-EGFP and Cx3cr1-RasV12 mice. Thus, Cx3cr1-RasV12 mice showed photoreceptor-specific degeneration.

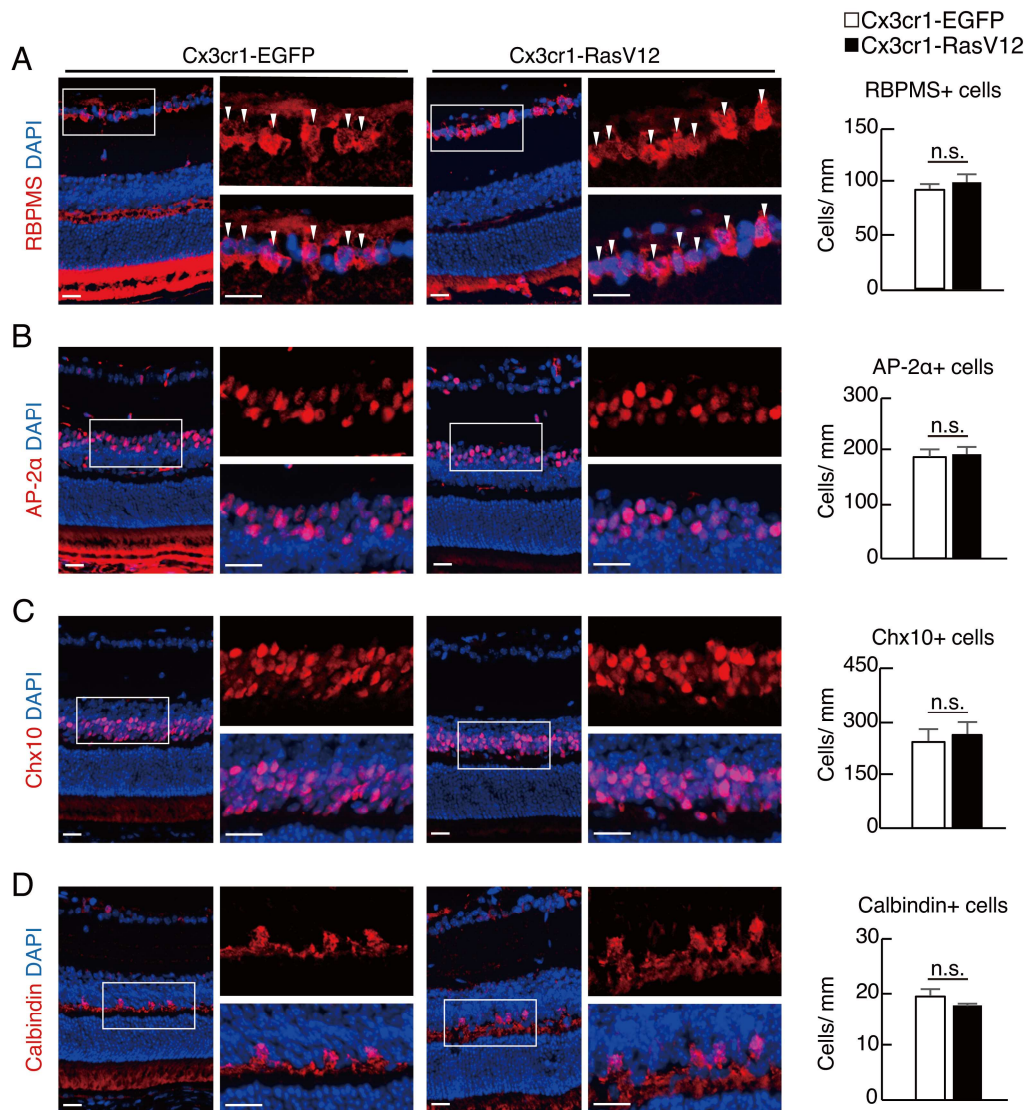


**Figure 17 Retinal ganglion cells, amacrine cells, bipolar cells, and horizontal cells were intact in the *Cx3cr1-RasV12* mice**

Staining results of (A) RBPMS (retinal ganglion cells), (B) AP-2α (Amacrine cells), (C) Chx10 (Bipolar cells), and (D) Calbindin (Horizontal cells) in retinal sections of Cx3cr1-EGFP or Cx3cr1-RasV12 mice at 7 days post-tamoxifen administration. The right graphs show the number of marker positive cells in the retina. in (A) White arrowheads indicate RBPMS-positive cells

Scale bars: (A-D), 20 μm. Data presented as mean with SEM. (n=6 per group, Mann-Whitney U test., n.s., not significant).



### ***RasV12-Expression in Microglia Aggravated N-Methyl-N-Nitrosourea-Induced Photoreceptor Degeneration***

RasV12-expression in microglia itself promoted photoreceptor degeneration in the retina. In this part, I investigated the role of RasV12-expressing microglia in photoreceptor degenerative conditions by using a pharmacological model. N-methyl-N-nitrosourea (MNU) is an alkylating agent, which can induce photoreceptor-specific apoptosis by injecting intraperitoneally in adult mice. MNU administrated mice are widely used as a retinitis pigmentosa model <sup>17</sup>. MNU (30 mg/kg) was intraperitoneally administered *Cx3cr1<sup>CreER/+</sup>* mice (Control) and *Cx3cr1-RasV12* mice at 2days after tamoxifen administration. Mice were sacrificed at 5 days post-MNU administration (7 days post-tamoxifen administration). DAPI staining revealed that the thickness of ONL became thinner in MNU treated *Cx3cr1-RasV12* (RasV12 +MNU) mice compared to MNU treated control (Control +MNU) mice (Fig. 18A, B). The thickness of ONL was reduced 4  $\mu$ m in RasV12 +MNU mice (Fig. 18B). The deficit of ONL cells was observed in nearby EGFP positive cells in RasV12 +MNU mice (Fig. 18C, D, arrowhead) Furthermore, transcripts of photoreceptor degeneration-related genes were significantly upregulated in RasV12 +MNU mice compared to control +MNU mice, suggesting that RasV12-expression in microglia aggravated photoreceptor degeneration induced by MNU.

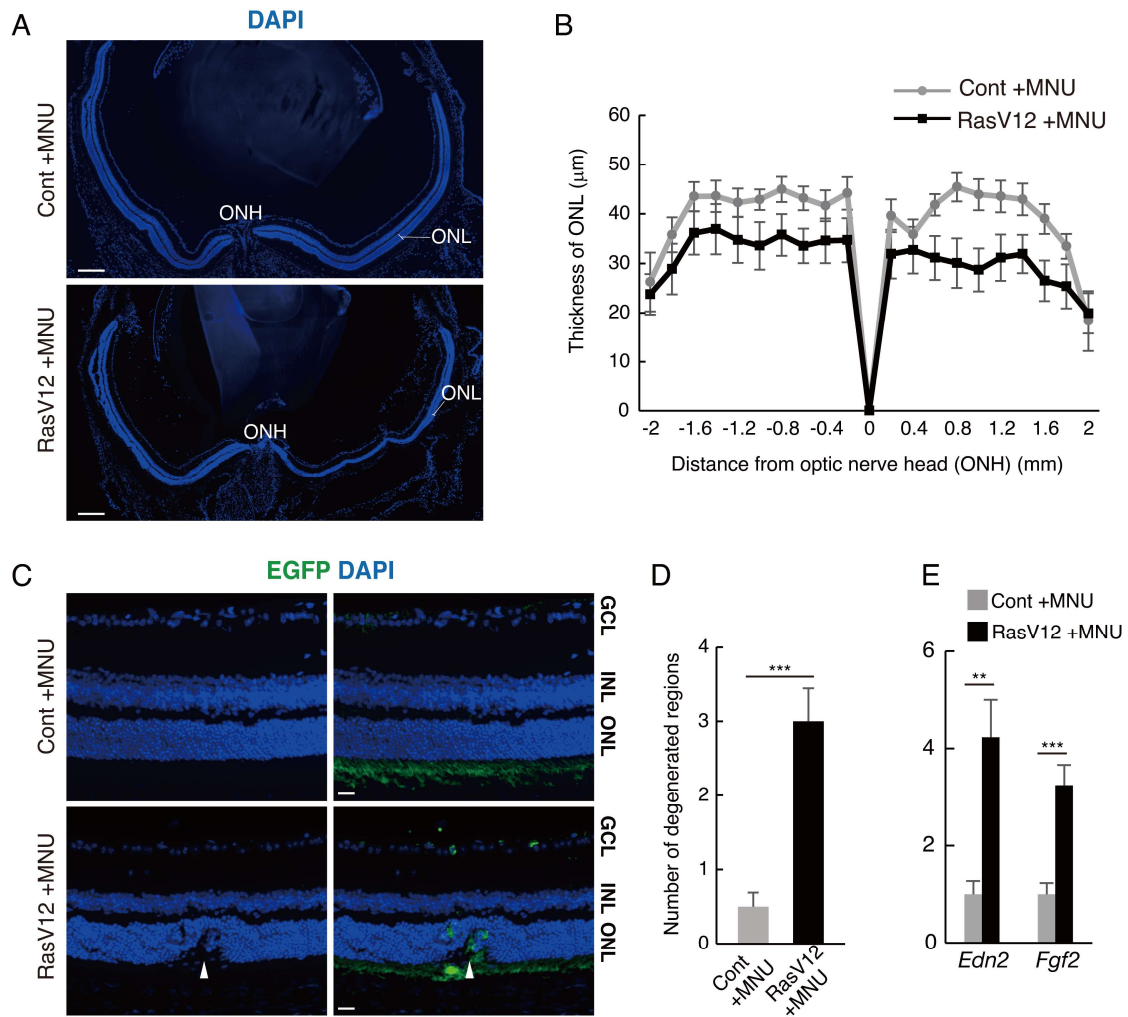


**Figure 18** The induction of photoreceptor degeneration by *N*-methyl-*N*-nitrosourea (MNU) in *Cx3cr1-RasV12* mice retina

(A) To analyze retinal cell layers, frozen sectioned retinas of MNU-treated *Cx3cr1<sup>CreET2R/+</sup>* mice (Cont +MNU) or MNU-treated *Cx3cr1-RasV12* mice (RasV12 +MNU) were subjected to DAPI staining at 5 days post-MNU administration (7 days post-tamoxifen administration). (B) The thickness of the ONL was measured from DAPI-stained pictures at 0.2 mm intervals. (C) Frozen sectioned retinas were subjected to immunohistochemistry using anti-EGFP antibody and nuclei were visualized by staining with DAPI. White arrowheads indicate the degenerative region in ONL. (D) The number of degenerative regions in ONL was counted. (E) Expression levels of *Edn2* and *Fgf2* transcripts by RT-qPCR in Cont +MNU and RasV12 +MNU mice.

Scale bars: (A), 200  $\mu\text{m}$ ., (C), 20  $\mu\text{m}$ . Data presented as mean with SEM. Asterisks indicate significant differences (Cont +MNU; n=8, RasV12 +MNU; n=14, Mann-Whitney U test., \*\*  $p < 0.01$ , \*\*\*  $p < 0.001$ ).

GCL; ganglion cell layer. INL; inner nuclear layer. ONL; outer nuclear layer. ONH; optic nerve head.

### ***Phagocytotic Activity and iNOS Expression of RasV12-Expressing Microglia***

RasV12-expressed microglia had Rhodopsin-positive regions in the cell body (Fig. 16B), suggesting that RasV12-expressing microglia phagocytosed photoreceptors. Z-stack analysis by confocal microscope showed that recoverin-positive rod photoreceptor was surrounded by EGFP-positive cells in Cx3cr1-RasV12 mice (Fig. 19A). To confirm the upregulation of phagocytotic activity, Cx3cr1-RasV12 retinas were immunostained with EGFP, Tmem119, and, a phagocytotic cell marker, CD68<sup>33, 66</sup>. (Fig. 19B-D). EGFP and Tmem119 double-positive cells strongly expressed CD68 in the ONL and SR at day 7 days post-tamoxifen administration in Cx3cr1-RasV12 mice (Fig. 19B, arrowheads). CD68 strongly expressed EGFP and Tmem119-positive cells were especially observed in the ONL in the Cx3cr1-RasV12 mice. (Fig. 19C). Also, the population of the CD68 strongly expressed EGFP and Tmem119-positive cells in the EGFP and Tmem119-double positive was high in the ONL and SR (Fig. 19D). More than 50% of EGFP and Tmem119-double positive were strongly expressed in the ONL and SR (Fig. 19D).

I checked the expression of phagocytosis-related genes by RT-qPCR. Expression of *C3* and *Cd68* was significantly upregulated in Cx3cr1-RasV12 mice compared with Cx3cr1-EGFP mice (Fig. 19E).

Activated microglia upregulates a nitric oxide (NO) synthetase, iNOS, and induces neuronal death by releasing NO that inducing oxidative stress to neurons<sup>67</sup>. Microglial iNOS expression was demonstrated in retinitis pigmentosa model mice<sup>59, 67</sup>, and an optic nerve injury mouse model<sup>69</sup>, suggesting that activated microglia induce retinal degeneration by upregulating iNOS expression. The expression of RasV12 induced iNOS expression in BV-2 microglial cells<sup>53</sup>. Immunohistochemical staining revealed strong iNOS expression in EGFP-positive microglial cells in Cx3cr1-RasV12 retinas (Fig. 19F). EGFP and iNOS double-positive cells were also observed in the inner retinal layers (Fig. 19F, G); nevertheless, this double-positive cell population was higher in the ONL and SR than in other regions of the retina (Fig. 19H).

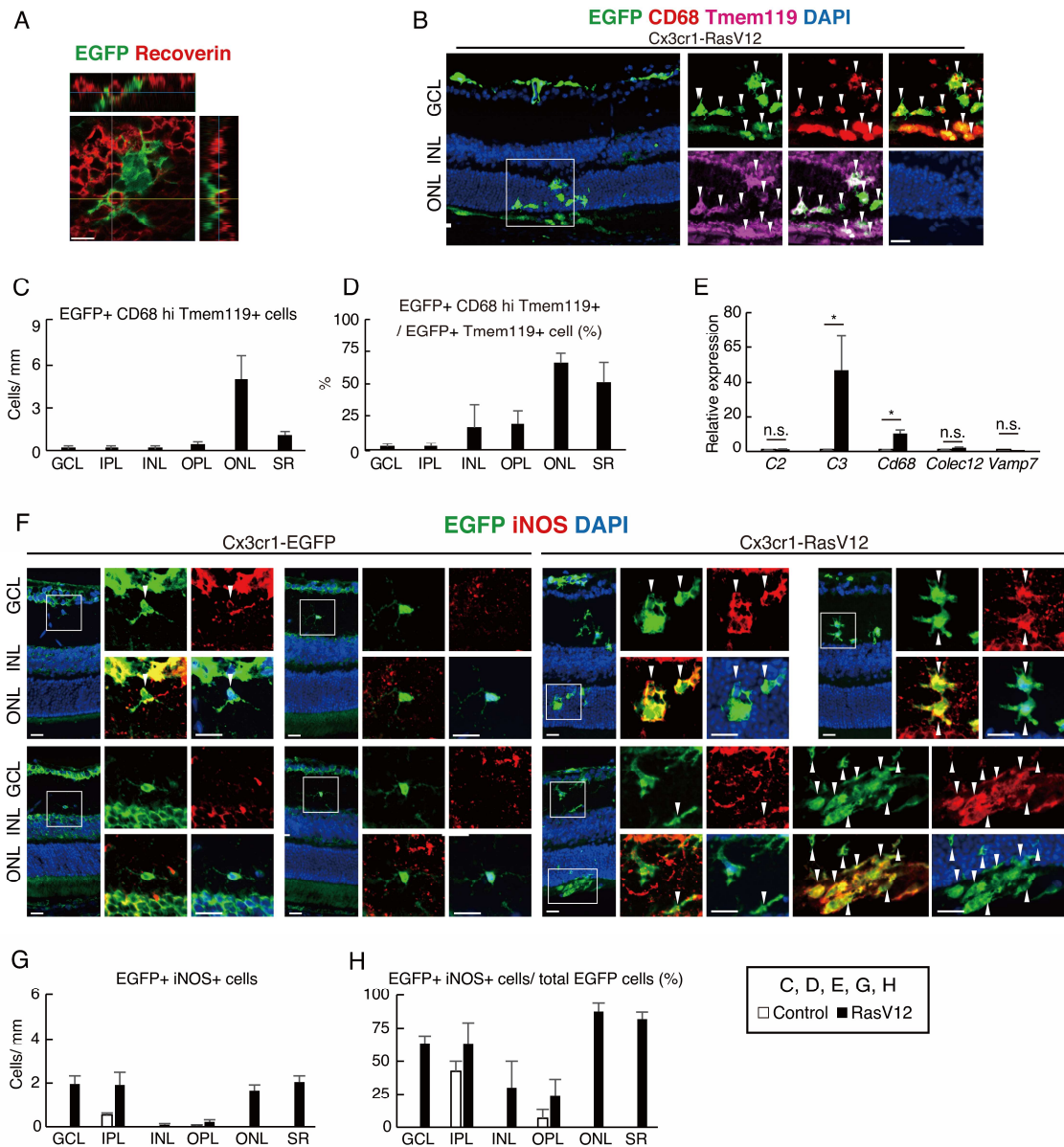


**Figure 19 Phagocytotic activity and iNOS expression of RasV12-expressing microglia**

(A) EGFP (Green) and Recoverin (Red) stained sections of Cx3cr1-RasV12 mice at 7 days post-tamoxifen administration. Z-stack pictures were acquired by a confocal microscope. Yellow, gray, and blue lines indicated X-, Y-, and Z-axes respectively. (B) EGFP (Green), CD68 (Red), and Tmem119 (Magenta) stained sections of Cx3cr1-EGFP or Cx3cr1-RasV12 mice at 7 days post-tamoxifen administration. White arrowheads indicate CD68 strongly expressing EGFP and Tmem119-triple positive cells. (C) The number of CD68 strongly expressing EGFP and Tmem119-triple positive cells in each

retinal layer. **(D)** The population of EGFP, CD68, and Tmem119-triple positive cells in the EGFP and Tmem119 double-positive cells in each retinal layer. **(E)** Gene expression patterns of phagocytosis-related genes in Cx3cr1-EGFP or Cx3cr1-RasV12 mice at 7 days post-tamoxifen administration. The gene expressions were quantified by RT-qPCR. **(F)** EGFP (Green) and iNOS (Red) stained sections of Cx3cr1-EGFP and Cx3cr1-RasV12 mice at 7 days post-tamoxifen administration. White arrowheads indicate EGFP and iNOS double-positive cells. **(F)** The number of EGFP and iNOS double-positive cells in each retinal layer. **(G)** The population of the EGFP and iNOS double-positive cells in the total EGFP positive cells in each retinal layer.

Scale bars: (A), 10  $\mu$ m., (B, F), 20  $\mu$ m. Data presented as mean with SEM. Asterisks indicate significant differences (n=6 per group, Mann-Whitney U test., \*  $p<0.05$ , n.s., not significant).

GCL; ganglion cell layer. IPL; inner plexiform layer. INL; inner nuclear layer. OPL; outer plexiform layer. ONL; outer nuclear layer. SR; subretinal regions

### ***The Cellular Kinetics of Ras-Activated Microglia Were Different Between the Inner and Outer Retina***

RasV12-expressing microglia had strong phagocytotic activity in the ONL and SR, indicating that photoreceptors were phagocytosed by RasV12-expressing microglia. I confirmed phagocytosis of photoreceptors by RasV12-expressing microglia using *ex vivo* confocal time-lapse imaging system. Isolated retinas from Cx3cr1-RasV12 were stained with Hoechst33342 to labeling the nuclei of retinas. EGFP-positive cells phagocytosed nuclei of photoreceptors (Fig. 20A) in the ONL, whereas did not show phagocytotic activities in the IPL (Fig. 20B), suggesting that RasV12-expressing microglia specifically phagocytosed photoreceptors and the cellular kinetics of Ras-activated microglia were different between the inner and outer retina.

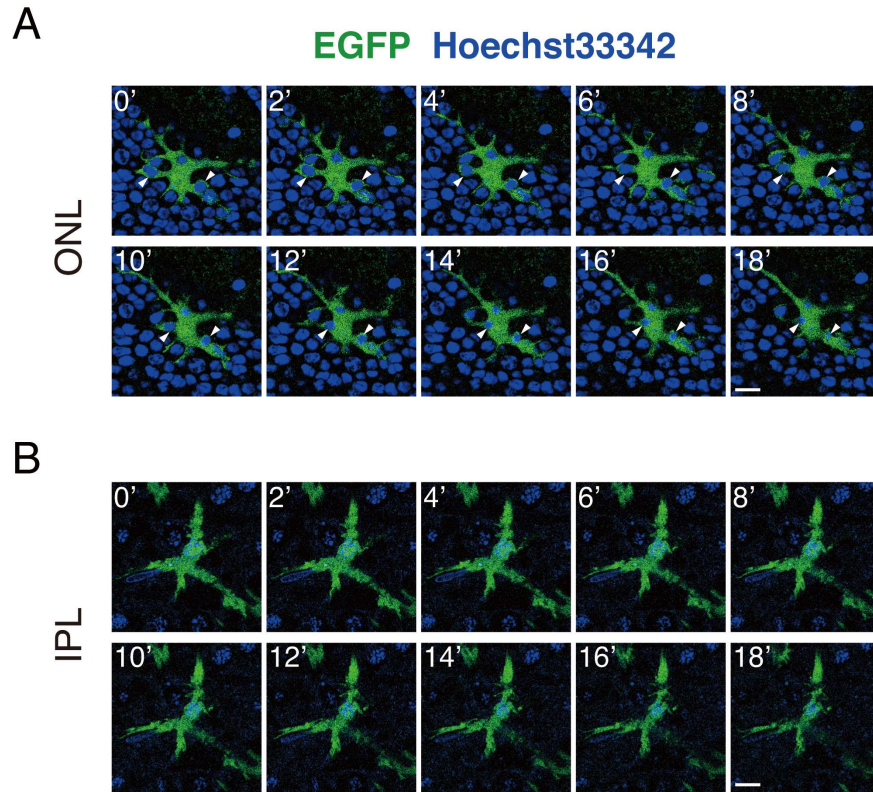


**Figure 20** *RasV12-expressing microglia phagocytosed nuclei in the ONL*

*Ex vivo* confocal time-lapse imaging analysis of Hoechst33342 stained Cx3cr1-RasV12 retina in the ONL and IPL. **(A)** In the ONL, EGFP-positive cell phagocytosed nuclei. White arrowheads indicate engulfing nucleus by EGFP-positive cells. **(B)** In the IPL, nucleus was not phagocytosed by EGFP-positive cell. Images are put in 2 minutes intervals. Scale bars: (A, B), 10  $\mu$ m.



### ***IL-33 May Modulate the Phenotype of Activated Microglia***

The degeneration was observed in the outer retina but not in the inner retina in Cx3cr1-RasV12 mice even though RasV12-expressing microglia existed in both the outer and inner retina. Furthermore, the cellular kinetics of RasV12-expressing microglia differs in the IPL and ONL, indicating that activated microglial phenotype was regulated by the retinal microenvironment. IL-33 is specifically expressing in Müller glia <sup>46</sup> (Fig. 7) and changes activated microglial phenotypes from neurotoxic to neuroprotective phenotype by upregulating anti-inflammatory factors (IL-10 and TGF- $\beta$ ) *in vitro* <sup>47</sup>. Therefore, I examined the effects of IL-33 for microglia *in vitro* and RasV12-expressing microglia *in vivo*. To examine IL-33 effects in *in vitro*, I employed a mouse MG5 microglial cell line. MG5 is established from brain microglia of *p53* knock out mice <sup>54</sup>. IL-33 treatment on MG5 significantly upregulated transcripts of *Il1b*, *Il6*, and *Tnf* (pro-inflammatory related genes) compared to non-treatment control, but did not change the gene expression of anti-inflammatory genes (Fig. 21A). To evaluate the effects of IL-33 on activated microglia, MG5 were treated with IL-33 and Lipid A. Lipid A treatment induces microglial activation and shifts microglial phenotype to neurotoxic phenotype via activation of Toll-like receptor 4 (TLR4) signaling. IL-33 and Lipid A co-treatment on MG5 showed that significantly downregulated *Tnf*, whereas likely upregulated *Il10* (anti-inflammatory related genes) compared to lipid A treated MG5 (Fig. 21B).

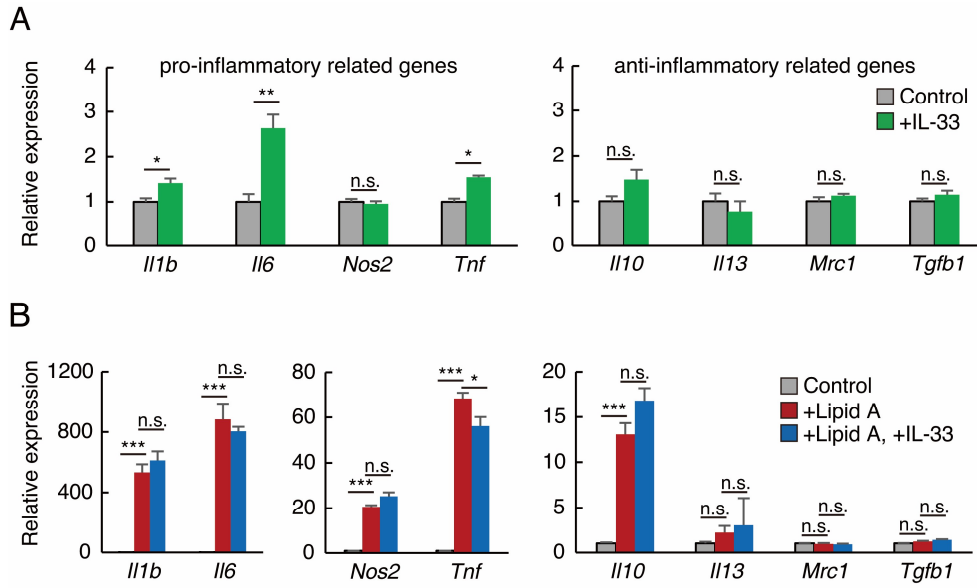


**Figure 21 Effects of IL-33 in mouse MG5 microglial cell line**

(A) IL-33 treatment on MG5. Expression of transcripts of pro- and anti-inflammatory related genes in non-treatment control and IL-33-treated MG5 were examined by RT-qPCR. (B) IL-33 and Lipid A treatment on MG5. Expression of transcripts of pro- and anti-inflammatory related genes in non-treatment control, Lipid A treatment, and IL-33 and Lipid A-treated MG5 were examined by RT-qPCR.

Data presented as mean with SEM. Asterisks indicate significant differences (in (A), n=4 per group, Mann-Whitney U test., in (B), n=4 per group One-way ANOVA Tukey-Kramer test., \*  $p < 0.05$ , \*\*  $p < 0.01$ , n.s., not significant).

Next, I confirmed IL-33 effects on RasV12-expressing microglia *in vivo*. IL-33 (500 ng) were intravitreally injected in right eye of Cx3cr1-RasV12 mice at 3 days post-tamoxifen administration. As a control, PBS was intravitreally administered in left eye of Cx3cr1-RasV12 mice or Cx3cr1-EGFP mice. Mice were sacrificed at 7 days post-tamoxifen administration. In IL-33 injected Cx3cr1-RasV12 mice, *Tgfb* expression was significantly upregulated compared to PBS injected Cx3cr1-RasV12 (Fig. 22A). However, IL-33 injection did not affect the distribution and number of RasV12-EGFP positive cells (Fig. 22B, C, D) and did not restore degenerative regions in ONL (Fig. 22E, F), and reduction in the thickness of the outer segments in Cx3cr1-RasV12 (Fig. 22 G, H).

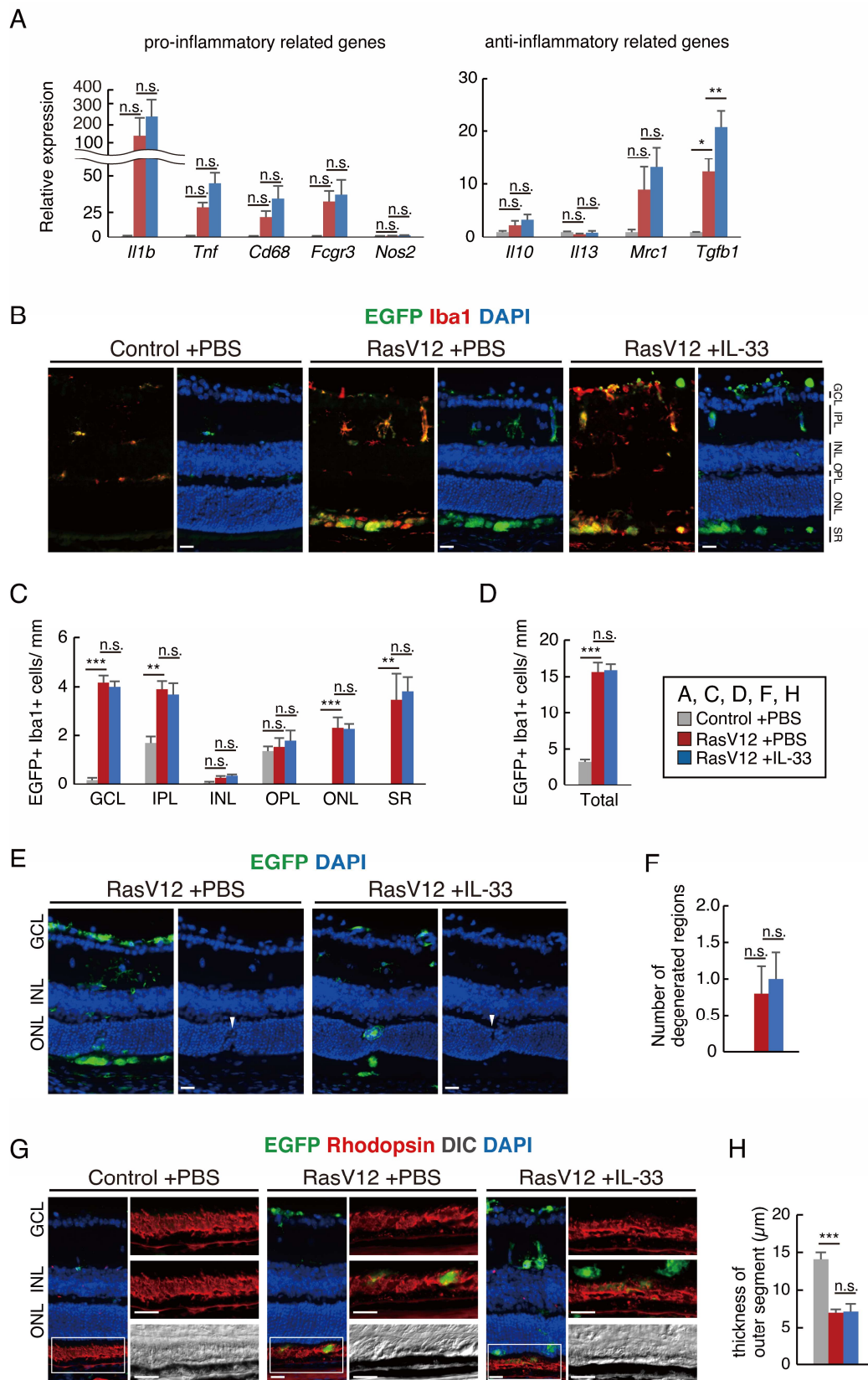


**Figure 22** Intravitreally injection of IL-33 in *Cx3cr1-RasV12* mice

IL-33 (500 ng) were intravitreally injected in the right eye of Cx3cr1-RasV12 mice (RasV12 +IL-33) at 3 days post-tamoxifen administration. As a control, PBS was intravitreally administered in the left eye of Cx3cr1-RasV12 mice (RasV12 +PBS) or Cx3cr1-EGFP mice (Control +PBS). Mice were sacrificed at 7 days post-tamoxifen administration. **(A)** Expression of transcripts of pro- and anti-inflammatory related genes in Control +PBS, RasV12 +PBS, and RasV12 +IL-33 were examined by RT-qPCR. **(B)** Frozen sectioned retinas of Control +PBS, RasV12 +PBS, or RasV12 +IL-33 were subjected to immunohistochemistry using anti-EGFP, -Iba1 antibody and nuclei were visualized by staining with DAPI. **(C)** The number of EGFP and Iba1 double positive cells in sub-regions of retina was counted. **(D)** The total number of EGFP and Iba1 double positive cells in the retina was counted. **(E)** Frozen sectioned retinas of control or Cx3cr1-RasV12 were subjected to immunohistochemistry using anti-EGFP and nuclei were visualized by staining with DAPI. White arrowheads indicate degenerative regions in the ONL. **(F)** The number of degenerative regions in the ONL was counted. **(G)** Frozen sectioned retinas of control or Cx3cr1-RasV12 were subjected to immunohistochemistry using anti-EGFP, -Rhodopsin antibody, and nuclei were visualized by staining with DAPI. Differential interference contrast (DIC) images are shown. **(E)** Thickness of outer-segment was measured from DIC pictures in control +PBS, RasV12 +IL-33, and RasV12 +IL-33 mice retina.

Scale bars: (B, E, G), 20  $\mu$ m. Data presented as mean with SEM. Asterisks indicate significant differences (Control +PBS; n=4, RasV12 +PBS and RasV12 +IL-33; n=7, One-way ANOVA Tukey-Kramer test., \*\* p< 0.01, \*\*\* p< 0.001).

GCL; ganglion cell layer. IPL; inner plexiform layer. INL; inner nuclear layer. OPL; outer plexiform layer. ONL; outer nuclear layer. SR; subretinal regions. Total; the total cell number of positive cells.

## Discussion

### ***Ras Activation in Microglia Activated Retinal Inflammatory Circuits by Inducing Photoreceptor Degeneration***

Previous studies tried to declare the roles of activated microglia in photoreceptor degenerative conditions using retinal degeneration models. However, it is still unclear that the roles of activated microglia in the early-onset of retinal degeneration because the retina has complex inflammatory circuits. Injured or degenerated photoreceptors secrete alarmins (e.g. endothelin-2: EDN2<sup>37</sup>, DAMPs, and ATP<sup>38</sup>) and activate Müller glia and microglia (Fig. 5). Previous studies are only cleared the activated microglial roles in late-onset retinal degenerative diseases. My microglial activation model via activating Ras signaling showed that inducing photoreceptor-specific degeneration, upregulation of photoreceptor degeneration related alarmin: *Edn2*, and activation of Müller glia. Therefore, activated microglia by Ras signaling induced photoreceptor degeneration and activation of retinal inflammatory circuits, indicating that activated microglia cue for activating of retinal inflammatory circuits and photoreceptor degeneration in the early-onset of retinal degeneration

### ***Ras Signaling Is Involved in Microglial Migration***

Ras-activated microglia detected and increased in both the GCL and ONL in Cx3cr1-RasV12 mice at 7 days post-tamoxifen administration, indicated that Ras-activated microglia migrated to the inner and outer retina. Because the Ras-MAPK signaling pathway activates cell migration-related downstream signaling pathways including MLCK, Paxillin, FAK, and Calpain<sup>70</sup>, Ras-activated microglia likely migrated by upregulating cell migration activity cell-autonomously, but directional characteristics of Ras-activated microglia was unclear.

### ***Mechanisms of Retina-Specific Degeneration in the Cx3cr1-RasV12 Mice***

Ras-activated microglia likely induced retinal degeneration by secreting cytotoxic factors and phagocytosing injured photoreceptors. Nitric oxide has been identified as one of the mediators of the cytotoxic effects of activated microglia <sup>71</sup>, and the expression of iNOS was upregulated by RasV12 expression in BV-2 <sup>53</sup>. Consistently, I observed enhanced expression of iNOS and inflammatory cytokines in RasV12-expressing microglia. These inflammatory stimuli may contribute to rod photoreceptor apoptosis and subsequent phagocytosis by RasV12-expressing microglia. Microglia are known to contribute to clearance of stressed photoreceptors by phagocytosis in rd10 mice <sup>32</sup>. Exposure of phosphatidylserine (PS) on the outer side of the cell membrane acts as an eat-me signal <sup>62</sup>. Milk fat globule-EGF factor 8 protein (MFG-E8) is secreted by activated microglia and leads to MFG-E8-PS complex formation <sup>72</sup>. Microglia recognizes MFG-E8-PS complex via integrin  $\alpha v \beta 3$  and starts phagocytosis of target cells <sup>73</sup>. Propidium Iodide (PI) negative Annexin V positive cells; PS-exposing live cells were specifically observed in CD73 positive fraction in Cx3cr1-RasV12 mice. Therefore, the specific occurrence of these events in rod photoreceptor may be one of mechanisms of specific damage of ONL.

RasV12 is likely expressed in the tissue-resident macrophage because Cx3cr1 is expressed in not only microglia but also tissue-resident macrophage, indicating that inflammatory mediators were secreted by non-CNS tissue-resident macrophage and induced photoreceptor degeneration. However, inflammatory mediators from non-CNS tissue were not likely to induce photoreceptor degeneration because RPE cells were intact in Cx3cr1-RasV12 mice.

The Cx3cr1-RasV12 mice showed retinal photoreceptor degeneration but did not show neurodegeneration in the brain. The retinal photoreceptors are transduced from light signal to electric signal via phototransduction cascade <sup>11</sup> and constitutively receiving

phototoxic damage, but the neurons in the brain are not constitutively receiving any damage. Therefore, retinal photoreceptors may have specifically induced degeneration by receiving light damage and Ras-activated microglia induced-inflammatory damages. Another hypothesis is that brain neurodegeneration was too early-onset to detected neurodegeneration by histological analysis

***Comparison of the Features Between Cx3cr1-RasV12 Mice, Retinitis Pigmentosa (RP) Model Mice, and RP Patients.***

Cx3cr1-RasV12 mice strongly induce microglial activation, but the degeneration level of photoreceptors was mild compared to RP model mice and RP patients because the ONL thickness is a single cell layer level in late-onset RP models and RP patient. Ras-activated microglia induced microglial proliferation, accumulation of microglia to the GCL and ONL, phagocytosis of photoreceptor, upregulation of inflammatory-related genes, and reduction of outer segment thickness in Cx3cr1-RasV12 mice. Moreover, Cx3cr1-RasV12 mice showed activation of Müller glial activation as characterized by GFAP expression. These phenotypes are shared between the Cx3cr1-RasV12 mice and RP model mice (rd10 mice <sup>32, 74</sup> and MNU-induced RP model <sup>75</sup>) except in accumulation of Ras-activated microglia in GCL and lack of ONL nucleus in Cx3cr1-RasV12 mice. In the human specimen, late-onset concentric RP patient shows that activated microglia accumulate in the ONL and SR especially photoreceptor degenerated regions, reduction of ONL thickness, and photoreceptor outer segments thickness <sup>14, 31</sup>. Cx3cr1-RasV12 mice shared phenotypes microglial accumulation of outer retina and reduction of photoreceptors with human RP patients. Thus, Cx3cr1-RasV12 mice are not adequate for the late-onset RP model but useful for the microglial activation model or microglia-induced early-onset retinal degeneration model.



### ***The Death of Cx3cr1-RasV12 Mice***

The Cx3cr1-RasV12 mice died on day 8~9 after tamoxifen treatment without showing neurodegeneration in the cerebrum and proliferation of CD11b positive cells in peripheral blood: leukemia-like phenotypes. RasV12 likely expressed in the tissue-resident macrophage because Cx3cr1 are expressing in not only microglia but also tissue-resident macrophage including alveolar macrophage (Lung), resident kidney macrophage, Kupffer cells (Liver) <sup>76</sup>. In the lung and liver, the induction of IL-1b and TNF- $\alpha$  involves in pulmonary fibrosis, pulmonary fibrosis, and cirrhosis <sup>77, 78, 79</sup>. Therefore, multiple organ failure and upregulation of inflammatory mediators in the whole body may contribute to the death of Cx3cr1-RasV12 mice. Future studies are required to examine the death of Cx3cr1-RasV12 mice.

### ***The Retinal Microenvironment May Regulate Microglial Activation and Phenotypes***

Cx3cr1-RasV12 mice showed photoreceptor-specific degeneration (lack of ONL nuclei and reduction of photoreceptor outer segments), and phosphatidylserine (PS) exclusively exposed on the cellular surface of CD73-positive rod photoreceptors, although iNOS upregulation was observed in RasV12-expressing microglia in both inner and outer sides of the retina. Furthermore, the cellular kinetics of Ras-activated microglia are different in the outer and inner sides of the retina. These results suggested that the microenvironment regulates microglial activation and phenotypes by extracellular factors.

IL-33 is expressing in homeostatic Müller glia <sup>46</sup> which especially expressing in the cell body and pseudopod inside of GCL, and is known to change activated microglial phenotypes from neurotoxic phenotype to neuroprotective phenotype by upregulating anti-inflammatory factors (IL-10 and TGF- $\beta$ ) *in vitro* <sup>47</sup>. I focused on IL-33 as a candidate factor that regulates neurotoxic phenotypes of RasV12-expressing microglia. Intravitreal injection of IL-33 in Cx3cr1-RasV12 upregulated *Tgfb1* (TGF- $\beta$ ) expression in Cx3cr1-

RasV12 retina. TGF- $\beta$  receptor signaling was reported to inhibit neurotoxic microglial activation<sup>80</sup>. Thus, IL-33 may regulate RasV12-expressing microglia by inducing TGF- $\beta$  expression. However, intravitreal injection of IL-33 did not restore RasV12-expressing microglial phenotypes such as upregulation of pro-inflammatory-related genes, abnormal distribution of microglia, and degeneration of photoreceptor. These results indicated that the effects of IL-33 in Cx3cr1-RasV12 mice were not detected at the histological level and constitutive activation of microglia by RasV12 expression exceeded IL-33-induced TGF- $\beta$  effects. Future studies are required to examine IL-33 effects in Cx3cr1-RasV12 mice by changing the administration method of IL-33 or dosage amount of IL-33.

IL-33-ST2L signaling induces leukocyte rolling by activation of endothelial cells accompanied by upregulating VCAM-1 in the brain<sup>81</sup>. Regulatory T (Treg) cells play a role in modulating the immune responses by secreting TGF- $\beta$ <sup>82</sup>. In retinopathy of prematurity inducing neovascularization, Treg cells are recruited into the retina and suppress retinal microglial activation<sup>83</sup>. On the other hand, macrophages can also express TGF- $\beta$  and have a role in tissue repair in non-CNS tissues<sup>84</sup>. The macrophages infiltrate from blood to the retina in the blood-retinal barrier (BRB) disordered conditions. Macrophages can infiltrate the retina in the age-related macular degeneration models that are accompanied by choroidal neovascularization<sup>85</sup>. These previous studies indicated that IL-33 may induce *Tgfb1* expression in the Cx3cr1-RasV12 mice by infiltrated immune cells from blood to the retina. However, all of the cells expressed, a microglia/macrophage marker, Iba1 near retinal capillary, and disordered of RPE cells and choroidal neovascularization were not detected in the IL-33 treated Cx3cr1-RasV12 mice. It is not likely that infiltrated immune cells and infiltrated immune cells contributed to the upregulating of *Tgfb1* in IL-33 treated Cx3cr1-RasV12 mice.

Another candidate factor is IL-34, which is produced by retinal ganglion cells <sup>21</sup>. IL-34 shows neuroprotective effects that prevent neurodegeneration from amyloid- $\beta$  in the microglia-neuron coculture model by inducing anti-oxidant factor, heme oxygenase 1 (HO-1) expression <sup>86</sup>. HO-1 attenuates the expression of proinflammatory genes including *Nos2* (*iNOS*), *Tnf*, and *Il6* in myeloid cells <sup>67</sup> and generates carbon monoxide (CO) <sup>87</sup>. HO-1/CO pathway inhibits LPS-induced phagocytotic activity of mouse BV-2 microglial cell line <sup>88</sup>. These reports indicated that IL-34 induced HO-1 expression in RasV12-expressing microglia in the IPL. In addition, HO-1 expression in RasV12-expressing microglia may show neuroprotective phenotypes by downregulating the expression of proinflammatory genes and phagocytotic activity in IPL. Thus, microglia suppressing condition in IPL may maintain by not only IL-33 but other factors including IL-34.

The other candidate factors are TGF- $\beta$  and CX3CL1. Lack of TGF- $\beta$  receptor in microglia cause degeneration of IPL and ONL by inducing apoptosis accompanied by microglial activation <sup>80</sup>. TGF- $\beta$  is expressing in the GCL and SR in intact retina <sup>89</sup>. On the other hand, CX3CL1-CX3CR1 signaling is well documented negative regulator for microglia which upregulates anti-inflammatory factors <sup>90</sup>. Furthermore, in the rd10 mice, CX3CR1 deficiency in microglia aggravates photoreceptor degeneration by increasing phagocytotic activity and inducing upregulation of inflammatory cytokines <sup>33, 91</sup>. CX3CL1 express in the GCL and INL but did not express in ONL in intact retina <sup>92</sup>. These studies suggest that TGF- $\beta$  and CX3CL1 constitutively expressing in the retina and negatively regulating microglia in homeostatic condition. CX3CL1, IL-34, and IL-33 are selectively expressing in the inner retina, suggesting that those factors are the most likely candidates which negatively regulated Ras-activated microglia in the inner retina. Future studies are necessary to examine the role of the immunosuppressive microenvironment of the inner side of the retina.

### ***Considerations for Differences of IL-33 Treatment Between In Vitro and In Vivo Models***

IL-33 treatment on MG5 significantly induced microglial *Il1b*, *Il6*, and *Tnf* (pro-inflammatory related genes) expression, but did not change the gene expression of anti-inflammatory genes unexpectedly. Moreover, IL-33 and Lipid A co-treatment on MG5 showed that significantly downregulated *Tnf*, whereas did not change the gene expression of anti-inflammatory genes. These results showed that the effect of IL-33 did not accord with *in vitro* and *in vivo* studies. There are two reasons why IL-33 effects were different between *in vitro* and *in vivo* models. First, as previously mentioned, the retina has complex inflammatory circuits. Indeed, the inflammatory circuits were activated in Cx3cr1-RasV12 mice suggesting that a lot of factors are multiply forming microglial phenotypes *in vivo* model, but components of *in vivo* model are few. Retinal neurons constitutively expressing microglia suppressing factors including CXCL1, IL-34, and TGF- $\beta$ <sup>21, 80, 93</sup>. The IL-33 may contribute neuroprotective effects by inducing *Tgfb1* expression *in vivo* situations. Second, because MG5 may have strongly activated and polarized inflammatory phenotypes by Lipid A treatment. co-treatment of IL-33 and Lipid A did not upregulate anti-inflammatory genes in the MG5. Lipid A or LPS-induced microglial activation models are widely using as *in vitro*. However, the question remains whether Lipid A or LPS-induced microglial activation models are mimicking microglial activation in neurodegeneration-induced microglial activation because Lipid A or LPS strongly activates via Toll-like receptor 4 (TLR4) signaling, and Lipid A and LPS did not exist in the CNS except gram-negative bacteria-infected condition.

IL-33 receptors consist of ST2L and IL-1 receptor accessory protein (IL1RAcP). ST2 has an extracellular domain that helps binding of IL-33 to IL1RAP and forming the IL-33-ST2L-IL1RAcP complex. The IL-33-receptor complex activates downstream signaling including NF- $\kappa$ B, MAPK, and p38 pathway via MyD88<sup>49</sup>. Expression of *St2l* and *Il1racp* are low in MG5 (Data was not showed), but the expression of inflammatory cytokines are

changed by IL-33 treatment on MG5, suggesting that MG5 are responded to IL-33 stimulation. Thus, it is unlikely that MG5 cannot receive IL-33 via its receptor and activate the receptor downstream signaling pathways.

### ***Microglial Activation May Trigger for the Pathogenesis of Photoreceptor Degenerative Diseases Including RP***

The age at onset of RP is middle age. Late-onset RP patients and animal models are accompanied by microglial activation in the photoreceptor degenerative regions <sup>15, 16, 31</sup>. In the aged mice retina, microglia are activated and accumulate in SR <sup>35</sup> and stimulate inflammatory pathways including IL-1, IL-3, and nitric oxide signaling. LPS-stimulated Ras-MAPK signaling pathway is also activated <sup>36</sup>. These studies suggested that age-related microglial activation is one of the key factors of RP development. My microglial activation model showed that strongly upregulated inflammatory factors including *C3*, *Il1b*, *Il6*, and *Tnf* expression and early-onset of photoreceptor degeneration. Therefore, microglia induced-inflammatory and -chronic inflammatory are triggers for the pathogenesis of photoreceptor degenerative diseases.

### ***Summary***

Ras-activated microglia induced upregulation of inflammatory mediators, increasing phagocytotic activities, activation of retinal inflammatory circuits, and photoreceptor-specific degeneration in the Cx3cr1-Ras mice. my study indicated that microglia-induced inflammatory is one of the triggers for the pathogenesis of neurodegenerative diseases including photoreceptor degenerative diseases. The Cx3cr1-RasV12 mice are useful for the microglial activation model or microglia-induced early-onset retinal degeneration model.

## Acknowledgments

I am grateful to Dr. Kaoru Uchimaru and Dr. Sumiko Watanabe for supervising and providing an opportunity for my Ph.D. studies. I thank Dr. Hideto Koso, Dr. Toshiro Iwagawa, Dr. Yukihiro Baba, and Ms. Asano Tsuhako for helpful discussions and suggestions. I thank Dr. Yasuyuki Fujita for providing *pCAG-LSL-RasV12-IRES-EGFP* mice strain. I also thank Dr. Mutsuhiro Takekawa, Dr. Ken Ishii, and Dr. Hiroshi Yotsuyanagi for fruitful advices and suggestions in the thesis defense.

## References

1. Kierdorf K, Prinz M. Microglia in steady state. *J Clin Invest*. 2017;127(9):3201-3209. doi:10.1172/JCI90602
2. Pixley FJ, Stanley ER. CSF-1 regulation of the wandering macrophage: Complexity in action. *Trends Cell Biol*. 2004;14(11):628-638. doi:10.1016/j.tcb.2004.09.016
3. Song X, Tanaka S, Cox D, Lee SC. Fcγ receptor signaling in primary human microglia: differential roles of PI-3K and Ras/ERK MAPK pathways in phagocytosis and chemokine induction. *J Leukoc Biol*. 2004;75(6):1147-1155. doi:10.1189/jlb.0403128
4. Colonna M, Wang Y. TREM2 variants: New keys to decipher Alzheimer disease pathogenesis. *Nat Rev Neurosci*. 2016;17(4):201-207. doi:10.1038/nrn.2016.7
5. Demb JB, Singer JH. Functional Circuitry of the Retina. *Annu Rev Vis Sci*. 2015;1:263-289. doi:10.1146/annurev-vision-082114-035334
6. Holtkamp GM, Kijlstra A, Peek R, De Vos AF. Retinal pigment epithelium-immune system interactions: Cytokine production and cytokine-induced changes. *Prog Retin Eye Res*. 2001;20(1):29-48. doi:10.1016/S1350-9462(00)00017-3
7. Streilein JW. Ocular immune privilege: the eye takes a dim but practical view of immunity and inflammation. *J Leukoc Biol*. 2003;74(2):179-185. doi:10.1189/jlb.1102574
8. Benhar I, London A, Schwartz M. The privileged immunity of immune privileged organs: The case of the eye. *Front Immunol*. 2012;3(SEP):1-6. doi:10.3389/fimmu.2012.00296
9. Zhou R, Caspi RR. Ocular immune privilege. *F1000 Biol Rep*. 2010;2(1):1-3. doi:10.3410/B2-3
10. Hosoya K ichi, Kubo Y. Vitamin Transport Across the Blood-Retinal Barrier: Focus on Vitamins C, E, and Biotin. In: *Handbook of Nutrition, Diet and the Eye*. ; 2014. doi:10.1016/B978-0-12-401717-7.00032-0
11. Klapper SD, Swiersy A, Bamberg E, Busskamp V. Biophysical properties of optogenetic tools and their application for vision restoration approaches. *Front Syst Neurosci*. 2016;10(SEP):1-14. doi:10.3389/fnsys.2016.00074
12. Organisciak DT, Vaughan DK. Retinal light damage: Mechanisms and protection. *Prog Retin Eye Res*. 2010;29(2):113-134. doi:10.1016/j.preteyeres.2009.11.004

13. Parmeggiani F, S. Sorrentino F, Ponzin D, Barbaro V, Ferrari S, Di Iorio E. Retinitis Pigmentosa: Genes and Disease Mechanisms. *Curr Genomics*. 2011;12(4):238-249. doi:10.2174/138920211795860107
14. Hartong D, Berson E, Dryja T. Retinitis pigmentosa Prevalence and inheritance patterns. *Lancet*. 2006;368:1795-1809. [https://ac.els-cdn.com/S0140673606697407/1-s2.0-S0140673606697407-main.pdf?\\_tid=26be6064-c3a4-11e7-b6bd-00000aacb35f&acdnat=1510049725\\_a881580f76b9dcba337a82cbae60ae14](https://ac.els-cdn.com/S0140673606697407/1-s2.0-S0140673606697407-main.pdf?_tid=26be6064-c3a4-11e7-b6bd-00000aacb35f&acdnat=1510049725_a881580f76b9dcba337a82cbae60ae14).
15. Tsujikawa M, Wada Y, Sukegawa M, et al. Age at onset curves of retinitis pigmentosa. *Arch Ophthalmol*. 2008;126(3):337-340. doi:10.1001/archophth.126.3.337
16. Na KH, Kim HJ, Kim KH, et al. Prevalence, Age at Diagnosis, Mortality, and Cause of Death in Retinitis Pigmentosa in Korea—A Nationwide Population-based Study. *Am J Ophthalmol*. 2017;176:157-165. doi:10.1016/j.ajo.2017.01.014
17. Nambu H, Yuge K, Nakajima M, et al. Morphologic characteristics of N-methyl-N-nitrosourea-induced retinal degeneration in C57BL mice. *Pathol Int*. 1997;47(6):377-383. doi:10.1111/j.1440-1827.1997.tb04511.x
18. Reisenhofer M, Pannicke T, Reichenbach A, Enzmann V. Characteristics of Müller glial cells in MNU-induced retinal degeneration. *Vis Neurosci*. 2016;33(2016):1-8. doi:10.1017/S0952523816000109
19. Gargini C, Terzibasi E, Mazzoni F, Strettoi E. Retinal organization in the retinal degeneration 10 (rd10) mutant mouse: A morphological and ERG study. *J Comp Neurol*. 2007;500(2):222-238. doi:10.1002/cne.21144
20. Chang B, Hawes NL, Hurd RE, Davisson MT, Nusinowitz S, Heckenlively JR. Retinal degeneration mutants in the mouse. *Vision Res*. 2002;42(4):517-525. doi:10.1016/S0042-6989(01)00146-8
21. O’Koren EG, Yu C, Klingeborn M, et al. Microglial Function Varies by Niche in Retinal Homeostasis and Degeneration. *Immunity*. 2019;in press:1-15. doi:10.1016/j.immuni.2019.02.007
22. Prinz M, Priller J. Microglia and brain macrophages in the molecular age: From origin to neuropsychiatric disease. *Nat Rev Neurosci*. 2014;15(5):300-312. doi:10.1038/nrn3722
23. Li L, Eter N, Heiduschka P. The microglia in healthy and diseased retina. *Exp Eye Res*. 2015;136:116-130. doi:10.1016/j.exer.2015.04.020
24. Silverman SM, Wong WT. Microglia in the Retina: Roles in Development, Maturity, and Disease. *Annu Rev Vis Sci*. 2018;4(1):45-77. doi:10.1146/annurev-vision-091517-034425
25. Schettters STT, Gomez-Nicola D, Garcia-Vallejo JJ, Van Kooyk Y. Neuroinflammation: Microglia and T cells get ready to tango. *Front Immunol*. 2018;8(JAN). doi:10.3389/fimmu.2017.01905
26. Scott G, Zetterberg H, Jolly A, et al. Minocycline reduces chronic microglial activation after brain trauma but increases neurodegeneration. *Brain*. 2018;141(2):459-471. doi:10.1093/brain/awx339
27. Nakagawa Y, Chiba K. Role of microglial M1/M2 polarization in relapse and remission of psychiatric disorders and diseases. *Pharmaceuticals*. 2014;7(12):1028-1048. doi:10.3390/ph7121028
28. Tang Y, Le W. Differential Roles of M1 and M2 Microglia in Neurodegenerative Diseases. *Mol Neurobiol*. 2016;53(2):1181-1194. doi:10.1007/s12035-014-9070-5
29. Ulland TK, Song WM, Huang SCC, et al. TREM2 Maintains Microglial Metabolic Fitness in Alzheimer’s Disease. *Cell*. 2017;170(4):649-663.e13. doi:10.1016/j.cell.2017.07.023

30. van Olst L, Verhaege D, Franssen M, et al. Microglial activation arises after aggregation of phosphorylated-tau in a neuron-specific P301S tauopathy mouse model. *Neurobiol Aging*. 2020;89:89-98. doi:10.1016/j.neurobiolaging.2020.01.003
31. Gupta N, Brown KE, Milam AH. Activated microglia in human retinitis pigmentosa, late-onset retinal degeneration, and age-related macular degeneration. *Exp Eye Res*. 2003;76(4):463-471. doi:10.1016/S0014-4835(02)00332-9
32. Zhao L, Zabel MK, Wang X, et al. Microglial phagocytosis of living photoreceptors contributes to inherited retinal degeneration. *EMBO Mol Med*. 2015;7(9):1179-1197. doi:10.15252/emmm.201505298
33. Tipoe GL, Wang K, Lin B, Xiao J, So K-F, Peng B. Suppression of Microglial Activation Is Neuroprotective in a Mouse Model of Human Retinitis Pigmentosa. *J Neurosci*. 2014;34(24):8139-8150. doi:10.1523/jneurosci.5200-13.2014
34. Norden DM, Godbout JP. Resistant to Regulation. *Neuropathol Appl Neurobiol*. 2014;39(1):19-34. doi:10.1111/j.1365-2990.2012.01306.x
35. Chen M, Xu H. Parainflammation, chronic inflammation, and age-related macular degeneration. *J Leukoc Biol*. 2015;98(5):713-725. doi:10.1189/jlb.3ri0615-239r
36. Ma W, Cojocaru R, Gotoh N, et al. Gene expression changes in aging retinal microglia: Relationship to microglial support functions and regulation of activation. *Neurobiol Aging*. 2013;34(10):2310-2321. doi:10.1016/j.neurobiolaging.2013.03.022
37. Rattner A. The Genomic Response to Retinal Disease and Injury: Evidence for Endothelin Signaling from Photoreceptors to Glia. *J Neurosci*. 2005;25(18):4540-4549. doi:10.1523/JNEUROSCI.0492-05.2005
38. Appelbaum T, Santana E, Aguirre GD. Strong upregulation of inflammatory genes accompanies photoreceptor demise in canine models of retinal degeneration. *PLoS One*. 2017;12(5):1-24. doi:10.1371/journal.pone.0177224
39. Joly S, Lange C, Thiersch M, Samardzija M, Grimm C. Leukemia Inhibitory Factor Extends the Lifespan of Injured Photoreceptors In Vivo. *J Neurosci*. 2008;28(51):13765-13774. doi:10.1523/JNEUROSCI.5114-08.2008
40. Ueki Y, Wang J, Chollangi S, Ash JD. STAT3 activation in photoreceptors by leukemia inhibitory factor is associated with protection from light damage. *J Neurochem*. 2008;105(3):784-796. doi:10.1111/j.1471-4159.2007.05180.x
41. Simanshu DK, Nissley D V., McCormick F. RAS Proteins and Their Regulators in Human Disease. *Cell*. 2017;170(1):17-33. doi:10.1016/j.cell.2017.06.009
42. Lim JKM, Leprivier G. The impact of oncogenic RAS on redox balance and implications for cancer development. *Cell Death Dis*. 2019;10(12). doi:10.1038/s41419-019-2192-y
43. Prior IA, Hood FE, Hartley JL. The Frequency of Ras Mutations in Cancer. *Cancer Res*. 2020;80(14):2969-2974. doi:10.1158/0008-5472.CAN-19-3682
44. Jurga AM, Paleczna M, Kuter KZ. Overview of General and Discriminating Markers of Differential Microglia Phenotypes. *Front Cell Neurosci*. 2020;14(August):1-18. doi:10.3389/fncel.2020.00198
45. Bennett ML, Bennett FC, Liddel SA, et al. New tools for studying microglia in the mouse and human CNS. *Proc Natl Acad Sci*. 2016;113(12):E1738-E1746. doi:10.1073/pnas.1525528113
46. Xi H, Katschke KJ, Li Y, et al. IL-33 amplifies an innate immune response in the degenerating retina. *J Exp Med*. 2016;213(2):189-207. doi:10.1084/jem.20150894
47. Yang Y, Liu H, Zhang H, et al. ST2/IL-33-dependent microglial response limits acute ischemic brain injury. *J Neurosci*. 2017;37(18):4692-4704. doi:10.1523/JNEUROSCI.3233-16.2017



48. Nguyen PT, Dorman LC, Pan S, et al. Microglial Remodeling of the Extracellular Matrix Promotes Synapse Plasticity. *Cell*. 2020;182(2):388-403.e15. doi:10.1016/j.cell.2020.05.050
49. Griesenauer B, Paczesny S. The ST2/IL-33 axis in immune cells during inflammatory diseases. *Front Immunol*. 2017;8(APR):1-17. doi:10.3389/fimmu.2017.00475
50. Yona S, Kim KW, Wolf Y, et al. Fate Mapping Reveals Origins and Dynamics of Monocytes and Tissue Macrophages under Homeostasis. *Immunity*. 2013;38(1):79-91. doi:10.1016/j.immuni.2012.12.001
51. Kawamoto S, Niwa H, Tashiro F, et al. A novel reporter mouse strain that expresses enhanced green fluorescent protein upon Cre-mediated recombination. *FEBS Lett*. 2000;470(3):263-268.
52. Kon S, Ishibashi K, Katoh H, et al. Cell competition with normal epithelial cells promotes apical extrusion of transformed cells through metabolic changes. *Nat Cell Biol*. 2017;19(5):530-541. doi:10.1038/ncb3509
53. Brahmachari S, Jana A, Pahan K. Sodium Benzoate, a Metabolite of Cinnamon and a Food Additive, Reduces Microglial and Astroglial Inflammatory Responses. *J Immunol*. 2009;183(9):5917-5927. doi:10.4049/jimmunol.0803336
54. Ohsawa K, Imai Y, Nakajima K, Kohsaka S. Generation and characterization of a microglial cell line, MG5, derived from a p53-deficient mouse. *Glia*. 1997;21(3):285-298. doi:10.1002/(SICI)1098-1136(199711)21:3<285::AID-GLIA4>3.0.CO;2-4
55. Koso H, Tshako A, Lai CY, et al. Conditional rod photoreceptor ablation reveals Sall1 as a microglial marker and regulator of microglial morphology in the retina. *Glia*. 2016;64(11):2005-2024. doi:10.1002/glia.23038
56. Wolf Y, Yona S, Kim K-W, Jung S. Microglia, seen from the CX3CR1 angle. *Front Cell Neurosci*. 2013;7(March):1-9. doi:10.3389/fncel.2013.00026
57. Landsman L, Liat BO, Zernecke A, et al. CX3CR1 is required for monocyte homeostasis and atherogenesis by promoting cell survival. *Blood*. 2009;113(4):963-972. doi:10.1182/blood-2008-07-170787
58. Rashid K, Akhtar-Schaefer I, Langmann T. Microglia in retinal degeneration. *Front Immunol*. 2019;10(AUG):1-19. doi:10.3389/fimmu.2019.01975
59. Prinz M, Erny D, Hagemeyer N. Ontogeny and homeostasis of CNS myeloid cells. *Nat Immunol*. 2017;18(4):385-392. doi:10.1038/ni.3703
60. Rathnasamy G, Foulds WS, Ling EA, Kaur C. Retinal microglia – A key player in healthy and diseased retina. *Prog Neurobiol*. 2018;(March):1-23. doi:10.1016/j.pneurobio.2018.05.006
61. Franco R, Fernández-Suárez D. Alternatively activated microglia and macrophages in the central nervous system. *Prog Neurobiol*. 2015;131:65-86. doi:10.1016/j.pneurobio.2015.05.003
62. Brown GC, Neher JJ. Microglial phagocytosis of live neurons. *Nat Publ Gr*. 2014;15(4):209-216. doi:10.1038/nrn3710
63. Koso H, Minami C, Tabata Y, et al. CD73, a novel cell surface antigen that characterizes retinal photoreceptor precursor cells. *Investig Ophthalmol Vis Sci*. 2009;50(11):5411-5418. doi:10.1167/iovs.08-3246
64. Vermes I, Haanen C, Steffens-Nakken H, Reutellingsperger C. A novel assay for apoptosis Flow cytometric detection of phosphatidylserine expression on early apoptotic cells using fluorescein labelled Annexin V. *J Immunol Methods*. 1995;184(1):39-51. doi:10.1016/0022-1759(95)00072-I
65. Ekstrom P, Sanyal S, Narfstrom K, Chader GJ, Van Veen T. Accumulation of glial fibrillary acidic protein in Muller radial glia during retinal degeneration. *Investig Ophthalmol Vis Sci*. 1988;29(9):1363-1371. doi:10.2307/3264029

66. Amadio S, Parisi C, Montilli C, Carrubba AS, Apolloni S, Volonté C. P2Yreceptor on the verge of a neuroinflammatory breakdown. *Mediators Inflamm.* 2014;2014. doi:10.1155/2014/975849
67. Brown GC. Nitric oxide and neuronal death. *Nitric Oxide - Biol Chem.* 2010;23(3):153-165. doi:10.1016/j.niox.2010.06.001
68. Aredo B, Zhang K, Chen X, Wang CXZ, Li T, Ufret-Vincenty RL. Differences in the distribution, phenotype and gene expression of subretinal microglia/macrophages in C57BL/6N (Crb1rd8/rd8) versus C57BL/6J (Crb1wt/wt) mice. *J Neuroinflammation.* 2015;12(1):4-17. doi:10.1186/s12974-014-0221-4
69. Noro T, Namekata K, Kimura A, et al. Spermidine promotes retinal ganglion cell survival and optic nerve regeneration in adult mice following optic nerve injury. *Cell Death Dis.* 2015;6(4):1-9. doi:10.1038/cddis.2015.93
70. Huang C. MAP kinases and cell migration. *J Cell Sci.* 2004;117(20):4619-4628. doi:10.1242/jcs.01481
71. Block ML. Neuroinflammation: Modulating mighty microglia. *Nat Chem Biol.* 2014;10(12):988-989. doi:10.1038/nchembio.1691
72. Fricker M, Neher JJ, Zhao J-W, Thery C, Tolkovsky AM, Brown GC. MFG-E8 Mediates Primary Phagocytosis of Viable Neurons during Neuroinflammation. *J Neurosci.* 2012;32(8):2657-2666. doi:10.1523/JNEUROSCI.4837-11.2012
73. Li E, Noda M, Doi Y, et al. The neuroprotective effects of milk fat globule-EGF factor 8 against oligomeric amyloid  $\beta$  toxicity. *J Neuroinflammation.* 2012;9:1-11. doi:10.1186/1742-2094-9-148
74. Roche SL, Ruiz-Lopez AM, Moloney JN, Byrne AM, Cotter TG. Microglial-induced Müller cell gliosis is attenuated by progesterone in a mouse model of retinitis pigmentosa. *Glia.* 2018;66(2):295-310. doi:10.1002/glia.23243
75. Zhang S, Zhang S, Gong W, et al. Müller Cell Regulated Microglial Activation and Migration in Rats With N-Methyl-N-Nitrosourea-Induced Retinal Degeneration. *Front Neurosci.* 2018;12(December):1-8. doi:10.3389/fnins.2018.00890
76. Mass E, Ballesteros I, Farlik M, et al. Specification of tissue-resident macrophages during organogenesis. *Science (80- ).* 2016;353(6304). doi:10.1126/science.aaf4238
77. Rabolli V, Badissi AA, Devosse R, et al. The alarmin IL-1 $\alpha$  is a master cytokine in acute lung inflammation induced by silica micro- and nanoparticles. *Part Fibre Toxicol.* 2014;11(1):1-15. doi:10.1186/s12989-014-0069-x
78. Oikonomou N, Harokopos V, Zalevsky J, et al. Soluble TNF mediates the transition from pulmonary inflammation to fibrosis. *PLoS One.* 2006;1(1). doi:10.1371/journal.pone.0000108
79. Lee M, Lee Y, Song J, Lee J, Chang SY. Tissue-specific role of CX3CR1 expressing immune cells and their relationships with human disease. *Immune Netw.* 2018;18(1):1-19. doi:10.4110/in.2018.18.e5
80. Ma W, Silverman SM, Zhao L, et al. Absence of TGF $\beta$  signaling in retinal microglia induces retinal degeneration and exacerbates choroidal neovascularization. *Elife.* 2019;8:1-28. doi:10.7554/eLife.42049
81. Cao K, Liao X, Lu J, et al. IL-33/ST2 plays a critical role in endothelial cell activation and microglia-mediated neuroinflammation modulation. *J Neuroinflammation.* 2018;15(1):1-12. doi:10.1186/s12974-018-1169-6
82. Wan YY, Flavell RA. "Yin-Yang" functions of transforming growth factor- $\beta$  and T regulatory cells in immune regulation. *Immunol Rev.* 2007;220(1):199-213. doi:10.1111/j.1600-065X.2007.00565.x
83. Deliyanti D, Talia DM, Zhu T, et al. Foxp3+ Tregs are recruited to the retina to repair pathological angiogenesis. *Nat Commun.* 2017;8(1):1-12. doi:10.1038/s41467-017-00751-w

84. Wynn TA, Vannella KM. Macrophages in Tissue Repair, Regeneration, and Fibrosis. *Immunity*. 2016;44(3):450-462. doi:10.1016/j.immuni.2016.02.015
85. Caicedo A, Espinosa-Heidmann DG, Piña Y, Hernandez EP, Cousins SW. Blood-derived macrophages infiltrate the retina and activate Muller glial cells under experimental choroidal neovascularization. *Exp Eye Res*. 2005;81(1):38-47. doi:10.1016/j.exer.2005.01.013
86. Mizuno T, Doi Y, Mizoguchi H, et al. Interleukin-34 selectively enhances the neuroprotective effects of microglia to attenuate oligomeric amyloid- $\beta$  neurotoxicity. *Am J Pathol*. 2011;179(4):2016-2027. doi:10.1016/j.ajpath.2011.06.011
87. Paine A, Eiz-Vesper B, Blasczyk R, Immenschuh S. Signaling to heme oxygenase-1 and its anti-inflammatory therapeutic potential. *Biochem Pharmacol*. 2010;80(12):1895-1903. doi:10.1016/j.bcp.2010.07.014
88. Scheiblich H, Bicker G. Regulation of microglial migration, phagocytosis, and neurite outgrowth by HO-1/CO signaling. *Dev Neurobiol*. 2015;75(8):854-876. doi:10.1002/dneu.22253
89. Wang X, Ma W, Han S, et al. TGF- $\beta$  participates choroid neovascularization through Smad2/3-VEGF/TNF- $\alpha$  signaling in mice with Laser-induced wet age-related macular degeneration. *Sci Rep*. 2017;7(1):1-13. doi:10.1038/s41598-017-10124-4
90. Sheridan GK, Murphy KJ. Neuron-glia crosstalk in health and disease: Fractalkine and CX3CR1 take centre stage. *Open Biol*. 2013;3(1 DEC). doi:10.1098/rsob.130181
91. Zabel MK, Zhao L, Zhang Y, et al. Microglial phagocytosis and activation underlying photoreceptor degeneration is regulated by CX3CL1-CX3CR1 signaling in a mouse model of retinitis pigmentosa. *Glia*. 2016;64(9):1479-1491. doi:10.1002/glia.23016
92. Zieger M, Ahnelt PK, Uhrin P. CX3CL1 (Fractalkine) protein expression in normal and degenerating mouse retina: In vivo studies. *PLoS One*. 2014;9(9). doi:10.1371/journal.pone.0106562
93. Zabel MK, Zhao L, Zhang Y, et al. Microglial phagocytosis and activation underlying photoreceptor degeneration is regulated by CX3CL1-CX3CR1 signaling in a mouse model of retinitis pigmentosa. *Glia*. 2016;64(9):1479-1491. doi:10.1002/glia.23016